UBIQUITIN-SPECIFIC PROTEASE 26 STABILIZES KINESIN FAMILY MEMBER 5B TO REGULATE MICROTUBULE DYNAMICS IN CASTRATION-RESISTANT PROSTATE CANCER

AN ABSTRACT

SUBMITTED ON THE FIRST DAY OF MAY 2024

TO GRADUATE PROGRAM IN BIOMEDICAL SCIENCES

IN PARTIAL FULFILLMENT OF THE REQUIREMENTS

OF THE SCHOOL OF MEDICINE

OF TULANE UNIVERSITY

FOR THE DEGREE

OF

MASTER OF SCIENCE IN ANATOMY RESEARCH

BY

KEYI SHEN

APPROVED:

Qiuyang Zhang, Ph.D.

Brian Rowan, Ph.D. Digitally signed by Brian Rowan, Ph.D. Date: 2024.05.07 15:43:40 -05'00'

Brian G. Rowan, Ph.D.

Wenke Feng, Ph.D.

Muralidharan Anbalagan, Ph.D.

ABSTRACT

Most of the Prostate Cancer (PCa) cases are managed by surgery, endocrine therapy (androgen-deprivation therapy, ADT), and chemotherapy. At certain stages of the treatment, some patients develop metastatic PCa with ADT resistance. This category of PCa is defined as metastatic Castration-Resistant Prostate Cancer (mCRPC). The last resort for mCRPC is chemotherapy. Once mCRPC develops chemotherapy resistance, it usually leads to an extremely poor prognosis and death. Thus, there is an urgent need to develop a novel treatment for mCRPC. Ubiquitin Specific Protease 26 (USP26), a deubiquitinase (DUB), reportedly promotes prostate cancer by inhibiting proteasomal degradation of androgen receptor (AR) and its constitutively active splice variant AR-V7. Whether USP26 regulates AR and AR-V7 signaling pathways by alternative mechanisms remains unclear. Previous studies indicate that changes in microtubule dynamics can spatially regulate AR signaling by alternating the nuclear translocation of AR. Our study focuses on the participation of USP26 in the microtubule dynamics.

USP26 was knocked down using small-interfering ribonucleic acid (siRNA) or a small hairpin ribonucleic acid (shRNA) lentiviral vector to facilitate loss-of-function studies. The cellular behaviors were analyzed with colony formation and cell proliferation assay. Fluorophore-tagged USP26 and its potential substrate, Kinesin Family Member 5B (KIF5B), were over-expressed to study their co-localization. Co-immunoprecipitation was used to estimate the ubiquitination level of KIF5B. Cycloheximide (CHX) chase assay was

carried out to analyze the KIF5B degradation under conditions with different USP26 levels. The expression of genes participating in the regulation of microtubule dynamics was analyzed with real-time quantitative Polymerase Chain Reaction (qPCR) and Western Blot (WB).

Our study indicates that USP26 co-localizes with KIF5B to cleave off lysine48 (K48)-linked ubiquitin chains from it. The deubiquitinated KIF5B is rescued from proteasomal degradation. The upregulated KIF5B promotes the phosphorylation of c-Jun N-terminal Kinase 2 (JNK2), a regulator of microtubule dynamics.

UBIQUITIN-SPECIFIC PROTEASE 26 STABILIZES KINESIN FAMILY MEMBER 5B TO REGULATE MICROTUBULE DYNAMICS IN CASTRATION-RESISTANT PROSTATE CANCER

A THESIS

SUBMITTED ON THE FIRST DAY OF MAY 2024

TO GRADUATE PROGRAM IN BIOMEDICAL SCIENCES

IN PARTIAL FULFILLMENT OF THE REQUIREMENTS

OF THE SCHOOL OF MEDICINE

OF TULANE UNIVERSITY

FOR THE DEGREE

OF

MASTER OF SCIENCE IN ANATOMY RESEARCH

BY

KEYI SHEN

APPROVED:

Qiuyang Zhang, Ph.D.

Brian Rowan, Ph.D.

Digitally signed by Brian Rowan, Ph.D.
Date: 2024.05.07 15:44:43 -05'00'

Brian G. Rowan, Ph.D.

Wenke Feng, Ph.D.

Muralidharan Anbalagan, Ph.D.

ACKNOWLEDGEMENT

I would like to express my gratitude to my supervisor, Dr. Qiuyang Zhang, for her time and effort devoted to my thesis. She guided me through the process of topic selection, research design, and manuscript preparation. She set a model for me that demonstrates the professionalism of a scientist. She taught me not only the sciences but also wisdom from her life experiences. Her support laid a solid foundation for my academic training at Tulane University.

I owe many thanks to our lab members. Dr. Sen Liu, our research scientist and lab manager, taught me the procedures of many experiments and their underlying mechanisms. Seleste Rivero, our technician, taught me Immunohistochemistry (IHC) and mouse genotyping procedures when I was rotating in Zhang Lab. Zixuan Li, our visiting scholar, helped me extract plasmids and took care of my cells when I was away for interviews. I may not have completed my training at Zhang Lab without their help.

I would also like to express my gratitude to my dissertation committee members. I was in the Histology class taught by Dr. Brian G. Rowan, Associate Professor and Chair of the Department of Structural and Cellular Biology. His teaching gave me basic knowledge and ignited my interest in biomedical sciences. Dr. Muralidharan Anbalagan, an assistant professor in the Department of Structural and Cellular Biology, taught me the procedures of cell culture and the skills that I need to work with nucleic acids. Dr. Wenke Feng, a professor in the Department of Structural and Cellular Biology, encouraged me to explore

and expand my knowledge in diverse fields. His encouragement gave me the strength to face challenges during my academic journey. Supports from the dissertation committee members were irreplaceable.

In addition, I owe my sincere gratitude to the remaining parts of the Department of Structural and Cellular Biology, especially the members of Dr. Zongbing You's lab and Dr. Brian G. Rowan's lab, where I completed my rotations. Dr. Zongbing You, a Professor and Vice Chair for Research in the Department of Structural and Cellular Biology, guided me through the Master of Science in Anatomy Research Program. His administrative role is greatly appreciated. His lab members, Dr. Sayed Ala Moududee (post-doctoral fellow) and Dr. Ben Jin (graduated Ph.D.), set great samples for me with their extraordinary pursuit of preciseness and rigorousness. On the other hand, Binghao Zou, a Ph.D. candidate from Dr. Brian G. Rowan's lab, inspired me to present my thesis in front of the dissertation committee with his impressive seminar. In addition, Ziqi Yang, a visiting scholar in Dr. Brain G. Rowan's lab, helped me learn to use the fluorescent microscope and develop my own imaging protocol for living cells. The Department of Structural and Cellular Biology is a highly supportive community. Their help made the completion of this thesis possible.

Finally, Figure 6 of Chapter I and Figures 1-2 of Chapter 2 were created with Biorender.com.

TABLE OF CONTENTS

LIST OF TABLES

I. UBIQUITIN-SPECIFIC PROTEASE 26 STABILIZES KINESIN FAMILY MEMBER 5B TO REGULATE MICROTUBULE DYNAMICS

II. LITERATURE REVIEW: NUCLEAR FACTOR KAPPA-B (NF-κB) REGULATION IN HUMAN CANCERS MEDIATED BY UBIQUITIN-SPECIFIC PROTEASES (USPs)

LIST OF FIGURES

I. UBIQUITIN-SPECIFIC PROTEASE 26 STABILIZES KINESIN FAMILY MEMBER 5B TO REGULATE MICROTUBULE DYNAMICS

II. LITERATURE REVIEW: NUCLEAR FACTOR KAPPA-B (NF-κB) REGULATION IN HUMAN CANCERS MEDIATED BY UBIQUITIN-SPECIFIC PROTEASES (USPs)

1. Introduction

1.1 Background

Among all cancers in men, prostate cancer (PCa) has the second-highest incidence rate and the fifth mortality rate worldwide [1]. Many of the death cases are associated with the development of resistance against androgen deprivation therapy (ADT) and chemotherapy. PCa with ADT resistance is defined as castration-resistant prostate cancer (CRPC). The last resort of CRPC is chemotherapy. Once the CRPC patient develops chemotherapy resistance, the prognosis is usually very poor. There is an urgent need to identify a novel treatment targeting a mechanism by which the CRPC develops and progresses. It has been reported that Ubiquitin-Specific Protease 26 (USP26) stabilizes Androgen Receptor (AR) and its constitutively active splice variant AR-V7 in CRPC to facilitate resistance against the androgen signaling inhibitors (AIS) [2]. Yet it is unknown whether USP26 can promote chemotherapy resistance through AR- or AR-V7-independent pathways. For instance, Docetaxel (DTX) is a common chemotherapy drug of CRPC targeting microtubules. It causes abnormal microtubule stabilization, which in turn leads to mitotic arrest and subsequent cellular death [3]. Our study focuses on the role of USP26 in the regulation of microtubule dynamics.

1.2 Knowledge Gap and Rationale

Ubiquitin was first discovered in the 1970s [4]. It is a protein consisting of 76 amino acid residues with a total molecular weight of 8.5 kDa. Seven of these amino acids are

lysine (K) residues (K6, K11, K27, K29, K33, K48, and K63) that determine the linking pattern of polyubiquitin chains and, therefore, dictate the destiny of the ubiquitinated protein [5]. Typical polyubiquitin chains linked by K48 and K63 residues are believed to be responsible for proteasomal degradation and signal transduction, respectively. Atypical polyubiquitin chains, such as K29 and K11, are associated with proteasomal degradation as well [5]. The remaining atypical polyubiquitin chains are mostly parts of the signaling pathways involving DNA repair and innate immune response [5].

The balance between ubiquitination and deubiquitination is essential for protein quality control and intracellular homeostasis [6-9]. Removal of the ubiquitin from its target protein requires a class of enzymes named deubiquitinases (DUBs). There are more than one hundred DUBs in humans in total. They can be divided into two classes – cysteine (also known as thiol) proteases and metalloproteases [10]. Cysteine proteases can be further divided into six superfamilies – the ubiquitin-specific proteases (USPs), the Machado-Josephin domain (MJDs) superfamily, the ubiquitin C-terminal hydrolases (UCHs), the K48-specific MIU-containing novel DUBs (MINDYs), ovarian tumor proteases (OTUs), and the K63-specific Zinc finger with Ubiquitin fold modifier (UFM)1-specific peptidase domain protein (ZUSFP) [10]. The USPs are the largest family of DUBs, with more than 60 members [11, 12]. They cleave off ubiquitin from their substrates, and deubiquitinated proteins can escape proteasomal degradation. The subtle balance between ubiquitination and deubiquitination controls the protein qualities and is important for the maintenance of cellular homeostasis.

USP26 is a member of the USP family. It first drew the attention of reproductive scientists because specific mutations in this gene were associated with male infertility [13].

Its role in cancer development and progression was not extensively studied until the recent decade. It has been validated that USP26 plays an essential role in the metastasis of esophageal squamous carcinoma and the progression of thyroid cancer by stabilizing Epithelial-to-Mesenchymal Transition (EMT) markers [14, 15]. Yet the role of USP26 in prostate cancer, especially in the mCRPC, remains to be investigated. Scientists' understanding of its role in prostate cancer was limited to its DUB activity that stabilizes androgen receptor (AR) and the constitutively active AR splice variant, AR-V7 [2, 16]. Whether USP26 can regulate the AR- or AR-V7 independent pathways remains unclear. In addition, a study on the membrane-associated AR implies that the spatial distribution of AR depends on the microtubule dynamics [17]. Whether USP26 participates in the regulation of microtubule dynamics is not known, either.

1.3 Objectives

1. To gain a preliminary understanding of USP26's role in PCa cellular behaviors such as colony formation and proliferation, we aim to knock down USP26 in PCa cells to test for changes in these behaviors.

2. KIF5B is a potential substrate of USP26 that passed the mass spectrometry screening. We aim to investigate whether KIF5B co-localizes with USP26 *in vitro*.

3. We aim to investigate the USP26's DUB activity against (the ubiquitinated) KIF5B and the potential consequences of deubiquitination.

4. We aim to investigate the role of USP26 in potential changes in the microtubule dynamics due to KIF5B's function as a microtubule regulator.

2. Materials and Methods

2.1 Materials

All the materials needed are listed in Table 2.

Table 1 **Materials**

Item No.	Product	Catalog No.	Manufacturer	Address
1	RPMI 1640 medium	25-506	Genesee Scientific	El Cajon, CA, USA
2	Dulbecco's Modified Eagle Medium (DMEM)	25-500	Genesee Scientific	El Cajon, CA, USA
3	DME/F12 1:1 medium	SH30023.01	HyClone Laboratories	Logan, UT, USA
4	1X OPTI-MEM	31985-070	Life Technologies Corporation	Grand Island, NY, USA
5	Phosphate Buffered Saline (PBS)	SH30256.01	HyClone Laboratories	Logan, UT, USA
6	Sterile-filtered Fetal Bovine Serum (FBS)	PS-FB3	Biowest USP, Inc.	Bradenton, FL, USA
7	100X Penicillin-Streptomycin (PS)	25-512	Genesee Scientific	El Cajon, CA, USA
8	0.05% trypsin	25-052-CI	Mediatech Inc.	Manassas, VA, USA
9	Lipofectamine 3000 transfection kit	L3000-015	Invitrogen (part of Thermo Fisher Scientific)	Carlsbad, CA, USA
10	PEI Prime linear polyethyleneimine	919012	Sigma-Aldrich Co.	St. Louis, MO, USA
11	CellTiter-Glo Substrate	G755A	Promega Corporation	Madison, WI, USA
12	Hoechst 33342	639	ImmunoChemistry Technologies, LLC	Bloomington, MN, USA
13	10X Radio Immuno-Precipitation Assay (RIPA) buffer	20-188	EMD Millipore Corp.	Billerica, MA, USA

14	Protease Inhibitor Cocktail (PIC)	P8340-5ML	Sigma-Aldrich Co.	St. Louis, MO, USA
15	Cytoplasmic and Nuclear Protein Extraction Kit	AR0106	Boster Biological Technology	Pleasanton, CA, USA
16	1X Quick Start Bradford Dye Reagent	5000205	Bio-Rad Laboratories, Inc.	Hercules, CA, USA
17	Direct-zol RNA Miniprep Plus	R2070	Zymo Research	Irvine, CA, USA
18	Plasmid Medi-prep	D4200	Zymo Research	Irvine, CA, USA
19	2X Universal SYBR Green Fast qPCR Mix	RM21203	ABclonal	Woburn, MA, USA
20	Retro-Transcription (RT) Reagent kit	RR037A	Takara Bio Inc.	San Jose, CA, USA
21	Acrylamide starter kit, 10%	161-0182	Bio-Rad Laboratories	Hercules, CA, USA
22	Mini PROTEAN Tetra System	1658004EDU	Bio-Rad Laboratories	Hercules, CA, USA
23	Semi-Dry Transfer Cell	1703940	Bio-Rad Laboratories	Hercules, CA, USA
24	Transfer membrane	IPFL00010	Merck Millipore Ltd	Tullagreen, Carrigtwohill, Ireland
25	10 ml serological pipets	12-104	Genesee Scientific	El Cajon, CA, USA
26	10 µl barrier tips	26-400	Genesee Scientific	El Cajon, CA, USA
27	200 µl barrier tips	24-412	Genesee Scientific	El Cajon, CA, USA
28	1000 µl barrier reach tips	24-430	Genesee Scientific	El Cajon, CA, USA
29	60 × 15 mm tissue culture dishes	25-260	Genesee Scientific	El Cajon, CA, USA
30	96-well tissue culture plates	25-109	Genesee Scientific	El Cajon, CA, USA
31	23 cm Cell Scraper	25-270	Genesee Scientific	El Cajon, CA, USA
32	1.7 ml microtubes	22-281	Genesee Scientific	El Cajon, CA, USA
33	90 mm tissue culture dishes	FB012923	Fisher Scientific	Pittsburgh, PA, USA
34	6-well tissue culture plates	FB012927	Fisher Scientific	Pittsburgh, PA, USA

35	untreated 96-well cell culture plate	701011	Nest Biotechnology Co., Ltd.	Wuxi, China
36	Hemacytometer	392626	Hausser Scientific	Horsham, PA, USA
37	50 ml conical tubes	06-443-18	Fisher Scientific	Pittsburgh, PA, USA
38	15 ml centrifuge tubes	28-101	Genesee Scientific	El Cajon, CA, USA

Notes for Handling and Storage

1. To ensure successful cell culture, the cell culture media listed in Table 1 (except for OPTI-MEM) were all fortified with 10% (v/v) FBS and 1% (v/v) PS, stored at 4ºC.

2. To ensure successful cell lysis and stabilize total cell lysates, the 10X RIPA buffer was diluted into 1X, fortified with 1% (v/v) PIC, and stored at -20ºC.

3. For the complete functionality of the Plasmid Medi-prep kit, the P1 reagent is stored at 4ºC. The P2 reagent is warmed up in a 37ºC water bath for 10 minutes before use. The DNA Wash Buffer 2 is mixed with 88 ml of 100% ethanol.

2.2 Plasmids, Primers, and Other Nucleic Acid Products

Human USP26-set siRNA/shRNA/RNAi Lentivector (Cat#: 49304091), human USP26 lentiviral vector (Cat#: 49304061), and scrambled siRNA/shRNA/RNAi Lentivector (Cat#: i000238c) were purchased from Applied Biological Materials (ABM) Inc., Richmond, BC, Canada. The target sequence inserted into the USP26 siRNA/shRNA/RNAi Lentivector was 5’-CGCTATAGCTTGAATGAGTTT-3’. A vacant vector was made from the human USP26 lentiviral vector purchased from ABM using an endonuclease (EcoRV) and a DNA ligase in Dr. Qiuyang (Lisa) Zhang’s Lab.

Quantitative Real-time PCR primers were (customized and) purchased from Eurofins Genomics LLC, Louisville, KY, USA.

The following plasmids were purchased from Addgene, Watertown, MA, USA:

1. pLV-KIF5B-Myc, Cat#: 186614

2. mCh-KIF5B*-strep, Cat#: 120164

2.3 Antibodies

All the antibodies needed are listed in Table 3.

Table 2. **Antibodies**

Item No.	Antigen	Catalog No.	Host Species	Dilution Ratio (WB)	Manufacturer	Address
1	USP26	A7999	Rabbit	1:500	ABclonal	Woburn, MA, USA
2	KIF5B	A15284	Rabbit	1:500	ABclonal	Woburn, MA, USA
3	JNK1	A23206	Rabbit	1:1000	ABclonal	Woburn, MA, USA
4	JNK2	A1251	Rabbit	1:1000	ABclonal	Woburn, MA, USA
5	phospho-JNK1/2/3	AP0276	Rabbit	1:1000	ABclonal	Woburn, MA, USA
6	Androgen Receptor	A19611	Rabbit	1:1000	ABclonal	Woburn, MA, USA
7	KLK3 (PSA)	A2052	Rabbit	1:500	ABclonal	Woburn, MA, USA
8	NKX3.1	A23480	Rabbit	1:500	ABclonal	Woburn, MA, USA
9	Myc tag	AE010	Mouse	1:2000	ABclonal	Woburn, MA, USA
10	KIF5B	LS-B2489	Goat	1:500	LifeSpan BioScience, Inc.	Shirley, MA, USA
11	phosphor-MAP1B	PA5-23014	Rabbit	1:1000	Invitrogen (part of Thermo Fisher Scientific)	Carlsbad, CA, USA

Notes for Handling and Storage

(1) The purchased stock solutions of the antibodies listed above were stored at -20ºC.

(2) For re-use and long-term preservation, the actively used antibodies were diluted by the ratios listed above, dissolved in Tris-Buffered Saline (TBS) fortified with 1% (w/w) Bovine Serum Albumin (BSA) and 0.05% (w/w) sodium azide (NaN_3).

2.4 Adhesive Cell Culture

Human prostate cancer cell lines (PC-3 and C4-2) and the immortalized human embryonic kidney cell line (HEK293T) were obtained from the American Type Culture Collection (Manassas, VA, USA).

To revive the frozen cells:

1. Let the frozen cells thaw in cryovials in a 37ºC water bath.

2. The water bath may last 1 or 2 minutes. Once the contents in the cryovials turned into fluid, they were removed from the water bath, and the surfaces of the cryovials were wiped with 70% ethanol. The cleaned cryovials were then transferred into a cell culture hood.

3. Inside the culture hood, use a 1000 μl pipet (and a barrier tip) to transfer the cells from the cryovial to a 90 mm cell culture dish with a pre-heated culture medium.

4. Gently swirl the culture dish to mix the cells with the medium.

5. Label the culture dish and put it into an incubator with a 37ºC and 5% CO_2 environment.

For subcultures:

1. Remove the medium from the cell culture dish.

2. Wash the cell culture with PBS to remove the residual medium.

3. Apply trypsin (1 ml for the 60 mm dish and 3 ml for the 90 mm dish). Incubate at 37ºC for one minute.

4. Add 1 ml of medium to each cell culture to inhibit the trypsin activity. Gently swirl the dish to mix the medium with the trypsin.

5. Some cells may remain attached to the dishes after the incubation. Resuspend them in the mixture of medium and trypsin by repeated pipetting. Transfer the resuspended cells to 50 ml conical tubes.

6. Centrifuge at 650 × g for five minutes.

7. Remove the supernatant by aspiration.

8. Resuspend the cells in the medium by repeated pipetting.

9. Distribute the resuspended cells into fresh cell culture dishes by a 1:2 or 1:3 ratio (One dish of 80% confluent cells may be passed to two or three fresh cell culture dishes).

2.5 Plasmid Preparation

Purchased plasmids may be delivered to the laboratory in the form of pure plasmids or bacterial stabs. Upon arrival, each form of plasmid is processed differently.

2.5.1 Pure Plasmids

Day 1

1. Mix the plasmids (≤200 ng) with one aliquot (approximately 10 µl) of DH5-α bacteria in a 1.7 ml microtube.

2. Set the microtube from step 1 on ice for 30 minutes.

3. Place the microtube from the previous steps in a 42ºC water bath for exactly 30 seconds.

4. Move the microtube back on ice. Incubate for two minutes.

5. Add 200 μl of LB broth. Shake for one hour at 250 rpm and 37ºC.

6. Transfer 50 μl of the liquid bacterial culture to an agar plate fortified with antibiotics (e.g., kanamycin or ampicillin, depending on the antibiotic-resistant gene carried by the plasmid) and spread it with a glass rod sterilized on a Bunsen burner.

7. Incubate overnight at 37ºC.

Day 2

1. Retrieve the agar plate from the 37ºC incubator.

2. Pick one colony from the plate with an iron loop sterilized on a Bunsen burner. Transfer the picked colony into a 15 ml centrifuge tube.

3. Add 3 ml of LB broth fortified with antibiotics (kanamycin: 50 μg/ml; ampicillin: 100 μg/ml). Shake for 8 hours at 250 rpm and 37ºC.

4. Transfer the 3 ml of bacterial culture into a bacterial culture flask. Add antibiotics-fortified LB broth to reach a total volume of 150 ml.

5. Shake the flask for 24 hours at 250 rpm and 37ºC.

Day 3

1. Transfer 900 μl of the liquid-phase bacterial culture into a 1.7 ml microtube.

2. Add 100 μl of DMSO and mix thoroughly by repeated pipetting.

3. Freeze the bacterial culture, stored at -80ºC.

4. Transfer the remaining bacterial culture into 50 ml conical tubes.

5. Centrifuge the bacterial culture at 2254 × g for 10 minutes.

6. Discard the supernatant. Open the Plasmid Medi-prep kit purchased from Zymo Research.

7. Add 4 ml of the P1 reagent from the Plasmid Medi-prep kit to each 50 ml conical tube containing the palates from step 6.

8. Vortex the 50 ml conical tubes to obtain a homogenous mixture.

9. Add 4 ml of the P2 reagent from the Plasmid Medi-prep kit to each 50 ml conical tube from step 8. Gently reverse each tube 8 times to mix the contents.

10. Add 4 ml of the P3 reagent from the Plasmid Medi-prep kit to each 50 ml conical tube from step 9. Gently reverse each tube 8 times to mix the contents. Make sure that precipitate forms and the content completely turns yellow-green.

11. Gently pour the content into a syringe filter from the kit. Push the content through the filter into a fresh 50 ml conical tube with a syringe plunger from the kit.

12. Add 12 ml of DNA binding buffer to the filtered solution containing plasmids from step 11.

13. Place the DNA-binding column from the kit and load the DNA-binding column with the mixture from step 12.

14. Centrifuge the columns at 500 × g for 2 minutes. Discard the flow-through. Repeat this step until the solution from step 12 has completely flown through the column.

15. Add 2 ml of DNA wash buffer 1 to each column. Centrifuge at 500 × g for 2 minutes. Discard the flow-through.

16. Add 2 ml of DNA wash buffer 2 to each column. Centrifuge at 500 × g for 2 minutes. Discard the flow-through. Repeat this step.

17. Place the column in a collection tube from the kit. Centrifuge at 10,000 × g for 1 minute to make sure there is no more wash buffer in the column.

18. Place the column in a 1.7 ml microtube. Add 200 µl of elution buffer to the column. Incubate at room temperature for 1 minute. Centrifuge at 10,000 × g for 1 minute.

19. Keep the flow-through and discard the column. Measure the concentration and purity with a spectrophotometer. Freeze the plasmid and store it at -20ºC.

2.5.2 Bacterial Stabs

Day 1

1. Pick one piece of agar from the bacterial stab with an iron loop sterilized on a Bunsen burner.

2. Place the piece of agar from step 1 in a 15 ml centrifuge tube. Add 3 ml of LB broth fortified with antibiotics (kanamycin: 50 µg/ml; ampicillin: 100 µg/ml). Shake for 8 hours at 250 rpm and 37ºC.

3. Transfer the 3 ml of bacterial culture into a bacterial culture flask. Add antibiotics-fortified LB broth to reach a total volume of 150 ml.

4. Shake the flask for 24 hours at 250 rpm and 37ºC.

Day2

Refer to Day 3 procedures for pure plasmids.

2.6 Transfection

Note: All the procedures listed below were performed in a cell culture hood.

1. Every 1 μg of plasmids is diluted by 50-150 μl of serum-free OPTI-MEM medium in a sterilized 1.7 ml microtube.

2. For each microgram of diluted plasmids, add 3 μl of PEI (1μg/μl) or 2 μl of Lipofectamine 3000 plus 2 μl of P3000 reagent (from the same kit).

3. Mix the diluted plasmids and transfection reagent by repeated pipetting. Incubate the mixture at room temperature for 30 minutes.

4. Transfer the solution into the culture dish using a pipet with an appropriate size.

5. Mix the plasmid-reagent mixture with the cell culture medium by gently swirling the culture dishes.

6. Carefully move the culture dishes back to the incubator (37 ºC, 5% CO_2).

The following steps are optional.

7. Change the medium at least 6 hours later if necessary.

8. Transfection efficiency could be assessed using a Nikon Ti microscope if the plasmid is carrying a sequence of a fluorescent tag.

2.7 Stable Cell Line Selection

1. Select stable cell lines with appropriate antibiotics in accordance with the specific plasmid information. Select the HEK293T and PC3 stable cell lines expressing shUSP26 and scrambled shRNA using puromycin at a concentration of 1-2 μg/ml. Puromycin treatment may last 2-3 weeks.

2. When the remaining cells form colonies of approximately 100 cells, apply trypsin to the colonies individually to detach the cells from the culture dishes. Transfer the detached cells to a 96-well plate.

3. As the selected cells proliferate, transfer them to 24, 12, and 6-well plates. Eventually, these cells would be placed in 60 mm and 90 mm culture dishes.

4. Puromycin resistance can always be checked under a Nikon Ti microscope with a fluorophore-exciting light source during this process because the puromycin-resistant gene carried by the plasmids was fused with a GFP gene.

2.8 Live Fluorescent Microscopy

1. Make the cells express the proteins of interest tagged with a fluorescent protein by transfection. Let the cells grow at 37ºC and 5% CO_2 for 24-36 hours.

2. Remove the cell culture medium by aspiration. Add 0.5% (v/v) Hoechst 33342 (dissolved in the cell culture medium) to stain the nucleus. Incubate at room temperature for 15 minutes.

3. Start imaging under the bright field mode with the 4X objective lens. Identify the cells and adjust the focus.

4. Switch to the fluorescent mode. Turn on the exciting laser, the wavelength of which depends on the type of fluorescent tag. Look for cells with intermediate levels of fluorescent signals. Adjust the focus again for optimal images.

5. Adjust the camera parameters and take pictures.

6. Take fluorescent pictures of the same area from different channels. Save the mono-channel pictures as well as the merged ones.

7. Repeat steps 2-6 for imaging with 10X, 20X, and 40X objective lenses.

2.9 Protein Extraction

2.9.1 Total Cell Lysis

Note that the entire procedure must be performed on ice or at 4ºC if it is not specified.

1. Remove the cell culture medium by aspiration.

2. Add an appropriate amount of PBS to the culture dish.

3. Scrape off the cells with a 23 cm cell scraper and then transfer them into a 1.7 ml microtube to centrifuge at 650 × g for 5 minutes.

4. Remove the supernatant by aspiration.

5. Add approximately 20-120 μl of RIPA buffer to the sample according to the volume of palate at the bottom.

6. Resuspend the cells in RIPA buffer by repetitive pipetting.

7. Sonicate the resuspended cells three times for 5 seconds.

8. Let the sonicated sample sit still on ice for 10 minutes.

9. Centrifuge the sample at 10,000 × g for 10 minutes.

10. Transfer the supernatant to a fresh 1.7 ml microtube and store it in a -80 ºC freezer if it is not going to be used immediately.

2.9.2 Cytoplasmic and Nuclear Extract

1. Refer to steps 1-4 of section 2.9.1.

2. For every 10 μl of pellets that remained, add 100 μl of pre-chilled Cytoplasmic Extraction Reagent (CER) A to the microtube.

3. Vortex the samples until the cells were resuspended homogeneously.

4. Incubate the homogeneous cell suspension on ice for 10 minutes.

5. For every 100 µl of CER A, add 5 µl of CER B to the sample.

6. Vortex the mixture at maximum speed for 5 seconds and incubate on ice for 1 minute.

7. Repeat step 6 without incubation. Centrifuge at 16,000 × g for 5 minutes. Transfer the supernatant to fresh pre-chilled microtubes. Store the aliquots at -80 ºC for future use.

8. For every 100 µl of CER A added to the sample in the previous steps, add 50 µl of Nuclear Extraction Reagent (NER) to the remaining nuclei-containing cell debris.

9. Vortex the sample at maximum speed until a homogeneous cell suspension is obtained.

10. Place the homogeneous cell suspension on ice and vortex it for 15 seconds every 10 minutes for a total of 40 minutes.

11. Centrifuge the sample at 16,000 × g for 5 minutes and transfer the supernatant to fresh pre-chilled microtubes. Store the aliquots at -80 ºC for future use.

2.10 Bradford Assay

1. Fill the wells in the untreated 96-well cell culture plate with 100 µl of Bradford dye reagent.

2. Aliquot and dilute the standard BSA solution (2 mg/ml) to create a standard curve (0.1, 0.2, 0.4, 0.8, 1.2, 1.6, and 2.0 mg/ml).

3. Dilute the protein samples by 1:10 and 1:20 ratios.

4. Add 5 µl of standard BSA solution or protein samples to wells with 100 µl of Bradford dye reagent to measure the absorbance of light with a 595 nm wavelength (A595). Repeat each measurement once to calculate the mean value.

5. Plot the A595 of the standard solutions with Microsoft Excel to create a quadratic regression curve.

6. Substitute the A595 of the diluted protein samples into the regression curve to calculate the concentrations if they fall within the range of the standard's A595 readings.

2.11 SDS-PAGE and Western Blot Analysis

2.11.1 Gel Preparation

1. Thoroughly mix equal volumes of resolving gel ingredients A and B (approximately 3 ml for each gel) from the acrylamide starter kit with 30 µl of 10% ammonium persulfate (APS) and 3 µl of tetramethylethylenediamine (TEMED).

2. Transfer the mixture into the space between 2 glass panels with a serological pipet before solidifying.

3. Add isopropanol (the gel mix from the previous step is insoluble in isopropanol) on top of the fluid to eliminate bubbles. Once the stacking gel solidifies, remove the isopropanol and store the resolving gel (along with the glass panels) in 1X running buffer at 4ºC.

4. On the day of the experiment, prepare the stacking gel using a similar method. Insert a comb into the stacking gel before the solidification to create wells where samples can be loaded.

Notes:

(1) Ingredient A (resolving gel) = 20% acrylamide stock solution

(2) Ingredient B (resolving gel) = Tris buffer, pH 8.8

(3) Ingredient A (stacking gel) = 10% acrylamide stock solution

(4) Ingredient B (resolving gel) = Tris buffer, pH 6.8

2.11.2 Sample Loading and Electrophoresis

1. Load equal amounts of protein samples from the same experiment.

2. Treat the samples with 5X loading buffer based on their volumes and heat to 95 ºC for 15 minutes. The treated samples were then ready for electrophoresis.

3. While the samples are being treated at 95 ºC, assemble the gel box and remove the comb from the stacking gel to create wells where samples will be loaded.

4. During the electrophoresis, run the samples through the stacking gel at 95 V for approximately 15 minutes and through the resolving gel at 120 V for 60 minutes.

5. While running the gel, activate the PVDF membrane with methanol. Soak both the activated PVDF membrane and filter papers in the transfer buffer for at least 30 minutes.

2.11.3 Transfer to PVDF Membrane

1. Remove the gel (along with the glass panels) from the gel box.

2. Remove the shorter glass panel.

3. Trim the gel. Discard the stacking gel. Trim the edges of the resolving gel to make it smooth.

4. Rinse the exposed gel with the transfer buffer before placing the PVDF membrane on top of the gel.

5. While placing the PVDF membrane, let one side of the membrane contact one edge of the gel before the remaining part of the membrane is gently laid down. This procedure was analogous to mounting a coverslip on a slide.

6. Once confirmed that there are no bubbles between the gel and the membrane, place a piece of filter paper on top of the PVDF membrane in a similar manner. At this moment,

the partly assembled transfer system (gel, PVDF membrane, and filter paper) is sitting on the taller glass panel.

7. Flip the assembly from step 6 and lay the side of the filter paper on a solid surface.

8. Gently remove the remaining glass panel (normally, the gel will separate from the glass spontaneously due to gravity as the glass is gently lifted, and no bubbles are supposed to pop up between the gel and the PVDF membrane).

9. Place a second piece of filter paper on the very top of the system, creating a sandwich-like structure. Use a roller to roll over the "sandwich" uni-directionally to eliminate potentially remaining air bubbles.

10. Place the "sandwich" in a BioRad semi-dry transfer cell. For a successful transfer, set up a constant voltage at 20V for 30 minutes.

2.11.4 Immunoblotting

1. Rinse the membrane with 1X Tris-Buffered-Saline-Tween 20 (TBST) immediately after the transfer.

2. Block with 5% (w/w) milk at room temperature for approximately one hour.

3. Rinse the blocked PVDF membrane with TBST.

4. The purchased primary antibodies should have been diluted using a ratio recommended by the manufacturer at this moment.

5. Seal the membrane in a plastic bag or place it in a dark plastic box with the desired primary antibody.

6. Incubate at room temperature for two hours or incubate at 4 ºC overnight.

7. Wash the PVDF membrane three times with TBST for 5 minutes.

8. Incubated with the secondary antibody that was specific to the host of the primary antibody. For the secondary antibody, incubation at room temperature would take only one hour, and incubation at 4 ºC would take overnight.

9. Wash the PVDF membrane three times in TBST for 5 minutes before scanning with a LI-COR scanner.

10. Repeat the incubating and washing procedures for each protein of interest.

Order of incubation:

(1) phosphorylated protein before total protein

(2) protein with low expression level before protein with high expression level

(3) protein of interest before loading control

2.12 Immunoprecipitation (IP)

1. Refer to the section on protein extraction (by total cell lysis).

2. Add 20 μl of protein G-conjugated beads and an appropriate amount of the antibody (according to the manufacturer's recommendation) to 300-1000 μg of protein sample. Mix them thoroughly by repeated pipetting.

3. Close the lid of the 1.7 ml microtube. Seal with parafilm.

4. Incubate overnight on a shaker in a 4ºC cold room.

5. Wash three times with pre-chilled PBS.

6. Add loading buffer directly to the beads. Heat up the sample and keep it at 95ºC for 15 minutes.

7. Load the sample. Proceed with SDS-PAGE and Western Blot.

2.13 Cycloheximide (CHX) Chase Assay

1. Seed the HEK293T cells stably expressing shRNA of human USP26 into four 90 mm tissue culture dishes, as well as the ones stably expressing scrambled shRNA.

2. After 24 hours of incubation at 37 ºC and 5% CO2, treat both groups with CHX at a concentration of 50 μg/ml for 0, 1, 2, and 4 hours.

3. Harvest the cells and extract proteins in the form of Total Cell Lysate (TCL).

4. Determine the protein concentrations with Bradford Assay.

5. Load 70 μg of protein into each well of the SDS polyacrylamide gel.

6. Refer to the procedures for SDS-PAGE and Western Blot.

7. Use Glyceraldehyde 3-phosphate dehydrogenase (GAPDH) as a loading control.

2.14 DUB Activity Test

1. Seed the HEK293T stable cell line expressing shRNA of human USP26 and the HEK293T stable cell line expressing scrambled shRNA into 90 mm tissue culture dishes. Incubate for 24 hours at 37ºC and 5% CO_2.

2. Co-transfect both cell lines with Myc-tagged KIF5B, HA-tagged wildtype ubiquitin, and the HA-tagged ubiquitin constructs with only one functional lysine residue (K48) as indicated in Figure 3. Incubate for 24 hours.

3. Treat all the cells with MG-132 (50 μM) for at least four hours.

4. Extract proteins with RIPA buffer and proceed with co-IP, where Myc-tagged KIF5B was used as the bait. The co-IP was then followed by WB analysis.

2.15 RNA Extraction and Quantitative Real-time PCR (qPCR)

2.15.1 RNA Extraction

1. Remove the cell culture medium.

2. Add 300 µl of Tri-zol reagent directly to each 60 mm cell culture dish to lyse the cells.

3. Scrape off the lysed cells with a 23 cm cell scraper.

4. Transfer the total cell lysate to an RNase-free 1.7 ml microtube and centrifuge at 13,000 × g for one minute.

5. Transfer the supernatant to a fresh RNase-free 1.7 ml microtube.

6. Add an equal volume of 100% ethanol (300 µl) to the supernatant and mix thoroughly by repeated pipetting.

7. Transfer the mixture from step 6 into a Zymo-Spin IIICG Column in a collection tube and centrifuge at 13,000 × g for one minute. Discard the flow-through.

8. To treat the sample (on the column) with DNase I, add 400 µl of RNA wash buffer to the column and centrifuge the sample at 13,000 × g for one minute.

9. Prepare the DNase I in an RNase-free 1.7 ml microtube by adding 75 µl of DNA digestion buffer to 5 µl of DNase I stock solution.

10. Add the mixture from step 9 to the column and incubate at room temperature for 15 minutes.

11. Add 400 µl of RNA pre-wash buffer to the column and centrifuge at 13,000 × g for one minute. Repeat once.

12. Add 700 µl of RNA wash buffer to the column and centrifuge at 13,000 × g for two minutes. Discard the flow-through.

13. Transfer the column to an RNase-free 1.7 ml microtube.

14. For elution, add 50-100 µl of RNase-free water to the column and centrifuge at 13,000 × g for one minute. Keep the flow-through in the 1.7 ml microtube.

15. Measure the concentration and purity of the RNA with a spectrophotometer. Aliquot, freeze, and store the remaining samples at -80ºC.

2.15.2 Retro-Transcription

1. Mix up to 1 µg of total RNA (sample) with 2 µl of 5X PrimeScript Buffer, 0.5 µl of PrimeScript RT Enzyme Mix I, 0.5 µl of 50 µM oligo dT Primer, and 2 µl of 100 µM random 6-mers in a 0.25 ml PCR tube.

2. Adjust the volume of this mixture to 10 µl by adding RNase-free water.

3. Centrifuge the mixture to ensure thorough mixing.

4. Place the PCR tubes on a thermocycler after centrifuging.

5. Program the thermocycler to bring the sample temperature to 37 ºC and keep it for 15 minutes to retro-transcribe the RNA, and then 85 ºC for 5 seconds to deactivate the reverse transcriptase.

6. Place the retro-transcription products (i.e. cDNA) on ice for immediate use or store it at -20ºC.

2.15.3 Realtime Quantitative PCR (qPCR)

1. Mix 2 µl of retro-transcription cDNA with 120-480 µl of SYBR Green reagent/enzyme mix.

2. Distribute exactly 5 µl of the mixture into each well of a 96-well qPCR plate.

3. Add 5 µl of 1 µM (forward and reverse) primers to each well. This experimental setup is triplicated for each gene of interest.

4. Seal the plate with a heat-resistant plastic membrane.

5. Centrifuge the sealed plate at 1000 × g for one minute to ensure thorough mixing.

6. Place the plate on a thermocycler equipped with a qPCR plate reader. The thermocycler was programmed as such:

Cycle 1: 95 ºC for 30 seconds

Cycle 2-41: 95 ºC for 5 seconds and 60 ºC for 30 seconds.

7. The entire process took approximately one hour. Save the data on a flash drive for statistical analysis with Microsoft Office Excel on a computer.

2.16 Colony Formation Assay

1. Seed the cell lines stably expressing shRNA of USP26 and scrambled shRNA in 60 mm cell culture dishes. Let the cells grow for 24 hours.

2. Remove the medium from the 60 mm cell culture dishes.

3. Wash the cell cultures with PBS to remove the residual medium.

4. Apply 1 ml of trypsin. Incubate at 37ºC for one minute.

5. Add 1 ml of medium to each cell culture to inhibit the trypsin activity. Gently swirl the dishes to mix the medium with the trypsin.

6. Some cells may remain attached to the dishes. Resuspend them in the mixture of medium and trypsin by repeated pipetting. Transfer the resuspended cells to 50 ml conical tubes.

7. Centrifuge at 650 × g for five minutes.

8. Remove the supernatant by aspiration.

9. Resuspend the cells in the medium.

10. Count the cell with a hemacytometer under a bright field microscope.

11. Calculate the number of cells per milliliter for each stable cell line.

12. Seed cells from each stable cell line into three wells of a 6-well plate. Each well should have 5000 cells.

13. Let the cells grow for 15 days.

14. Remove the medium by aspiration. Wash with PBS.

15. Fix the cells with methanol.

16. Stain the cells with crystal violet dye. Let the dye immerse the cells for 15 minutes.

17. Wash off excessive dye by gently swirling the 6-well plate in a bucket of tap water.

18. Count the number of colonies for each cell line. Proceed with statistical analysis.

2.17 CellTiter-Glo Luminescent Proliferation Assay

1. Seed the human CRPC cells into 60 × 15 mm tissue culture dishes (1:3 ratio subculture) and incubate at 37 ºC with 5% CO_2 for 24 hours.

2. Transfect the cells in one dish with human USP26 siRNA (siUSP26) and cells in another dish with non-targeting RNA (siCTRL).

2. Incubate both siUSP26- and siCTRL-treated cells at 37 ºC with 5% CO_2 for 24 hours, then pass them into a 96-well plate with a density of 5000 cells per well.

3. Add 50 μl of CellTiter-Glo substrate to 3 wells and incubate for 10 minutes. Obtain the luminescence reading from a CLARIOstar Plus Microplate Reader and calculate for an average of a 0-hour baseline.

4. Repeat the CellTiter-Glo substrate treatment and luminescence reading procedure in 48 hours.

2.18 Statistical Analysis

Student's T-test was performed to detect significant differences between samples with or without USP26 knocked down.

3. Results

3.1 Mass Spectrometry (MS) Screening identifies potential substrates of USP26

To investigate the functions of USP26, a DUB, it is necessary to identify its substrates. Under physiological conditions, an enzyme may have a large number of substrates, making it impossible to test each enzyme-substrate interaction individually. Thus, Co-immunoprecipitation was performed using USP26 as the bait, and the sample was sent out for Mass Spectrometry screening. Proteins most likely to be a substrate of USP26 are listed in Table 1, among which the Kinesin Family Member 5B (KIF5B) was chosen to be investigated.

Table 3. **Mass Spectrometry Screening Result**

Gene Symbol	Coverage [%]	# Peptides	# PSMs	# Unique Peptides	Abundance Ratio: (Sample) / (Control)	Abundance Ratio Adj. P-Value
KIF5B	18	14	15	14	100	8.8489E-17
WDHD1	14	13	17	13	100	8.8489E-17
IGHG1	14	5	26	5	100	8.8489E-17
TIMM44	9	4	5	4	100	8.8489E-17
LAMC1	3	4	4	4	100	8.8489E-17
S100A7	36	4	5	4	100	8.8489E-17
ERLIN1	23	8	12	3	100	8.8489E-17
CYB5A	36	3	5	3	100	8.8489E-17
HAX1	13	3	5	3	100	8.8489E-17
TPR	2	3	3	3	100	8.8489E-17
BCS1L	25	3	3	3	100	8.8489E-17
ARHGAP29	3	3	3	3	100	8.8489E-17
CAMK2B	5	3	3	3	100	8.8489E-17
PA2G4	12	3	3	3	100	8.8489E-17

MRPL24	14	2	3	2	100	8.8489E-17
EBP	13	2	2	2	100	8.8489E-17
CHP1	13	2	2	2	100	8.8489E-17
PTRH2	19	2	2	2	100	8.8489E-17
NOP16	14	2	2	2	100	8.8489E-17
EIF4E2	13	2	2	2	100	8.8489E-17
MRFAP1	27	2	2	2	100	8.8489E-17
SIGMAR1	9	2	3	2	100	8.8489E-17
PPP6C	8	2	3	2	100	8.8489E-17
COQ6	20	2	2	2	100	8.8489E-17
ZNF24	6	2	2	2	100	8.8489E-17
CCDC47	12	2	2	2	100	8.8489E-17
C4orf3	36	2	3	2	100	8.8489E-17
ALDH1A1	4	2	2	2	100	8.8489E-17
DTYMK	11	2	2	2	100	8.8489E-17
MCTP2	2	2	2	2	100	8.8489E-17
MRPS16	26	2	3	2	100	8.8489E-17
UQCR10	38	2	3	2	100	8.8489E-17
CRYZ	11	2	2	2	100	8.8489E-17
PPP2R5E	5	2	2	2	100	8.8489E-17
ARPC4	11	2	2	2	100	8.8489E-17
CCDC51	4	2	2	2	100	8.8489E-17
MTX3	6	2	2	2	100	8.8489E-17
BCLAF1	45	50	218	1	100	8.8489E-17
KRT6B	42	30	121	1	100	8.8489E-17
RPS18	97	4	18	1	100	8.8489E-17
C5	2	4	7	1	100	8.8489E-17
HBA2; HBA1	22	3	14	1	100	8.8489E-17
PHLDB3	7	1	3	1	100	8.8489E-17
IGKV1-27	14	1	4	1	100	8.8489E-17
PDCD6	9	1	2	1	100	8.8489E-17
RPLP1	14	1	2	1	100	8.8489E-17
IGLV4-60	8	1	14	1	100	8.8489E-17
NIP7	8	1	3	1	100	8.8489E-17
ACAA1	3	1	2	1	100	8.8489E-17
MRPL33	17	1	2	1	100	8.8489E-17
NUDT8	4	1	2	1	100	8.8489E-17

3.2 Knockdown of USP26 inhibits cell proliferation

To investigate the influence of USP26 on cellular behaviors, a colony formation assay, a cell proliferation assay, and a cell migration assay were carried out. It was readily visible that the PC3 cells with USP26 stably knocked down formed fewer colonies on average, yet no significant differences were detected (p=0.06, Figure 1A-1C). The proliferation rate is significantly downregulated as USP26 was knocked down by siRNA (Figure 1C). There is no evidence that knockdown of USP26 by siRNA can lead to significant changes in the migration rate (p = 0.27, Figure 1D-1E).

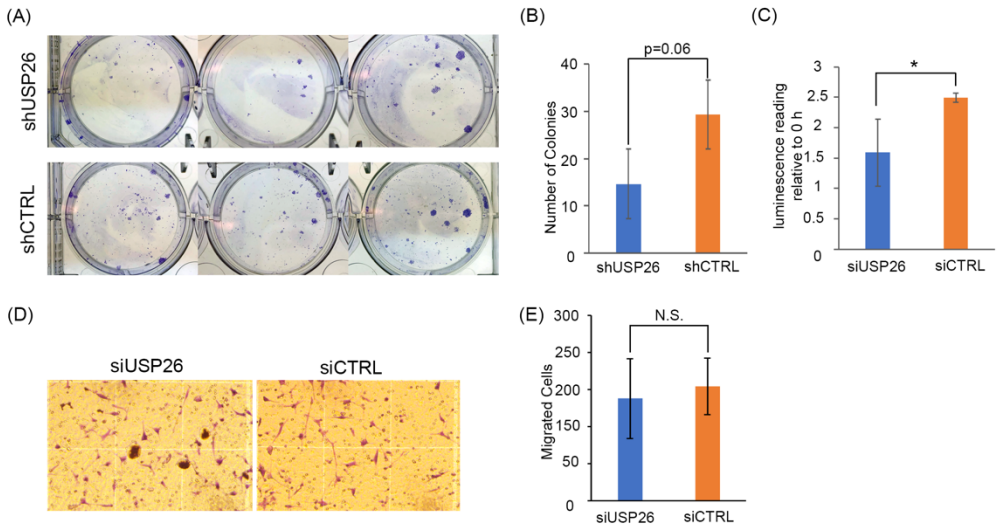

Figure 1**. Knockdown of USP26 is associated with inhibited cell proliferation.** (A) PC3 stable cell lines expressing shRNA of human USP26 and the PC3 cell line expressing scrambled shRNA were seeded into a 6-well plate. The initial cell density was 5000 cells per well. Cells were fixed with methanol and stained with crystal violet dye after 15 days of incubation at 37ºC and 5% CO_2. (B) Statistical Analysis of (A). (C) PC3 cells were seeded into a 96-well tissue culture plate. The initial density was 5000 cells per well. On

Day 1, Cells were transfected with siRNA of human USP26 ("siUSP26") and non-targeting siRNA ("siCTRL"), and luminescent reading was measured as described in the chapter on Materials and Methods. On Day 3, the luminescent reading was measured again. Y-axis labels stand for the luminescent reading relative to the Day 1 baseline. Error bars stand for the 95% confidence interval (D) C4-2 cells were transfected with siRNA of human USP26 ("siUSP26") and non-targeting siRNA ("siCTRL"). After 24 hours of incubation at 37ºC and 5% CO_2, 5000 cells from each sample were seeded into each well in a trans-well plate. Each well was filled with 600 μl of medium with 10% fetal bovine serum (FBS) below the trans-well device, and each trans-well device was filled with the FBS-free medium. After 4 hours of incubation at 37ºC and 5% CO_2, the cells were fixed with methanol and stained with crystal violet, followed by statistical analysis. Error bars stand for the 95% confidence interval. (E) Statistical Analysis of (D). The asterisks stand for significant differences (*: $p < 0.05$; **: $p < 0.01$; ***: $p < 0.001$; N.S: No Significance).

3.3 USP26 and KIF5B co-localizes in CRPC cells

To investigate whether an enzyme interacts with a potential substrate, PC3 cells were co-transfected with eGFP-USP26 and mCh-KIF5B (truncated motor domain, amino acids 1-555) and proceeded with live fluorescent microscopy. Once taken, images with Green Fluorescent Protein (GFP) signals and images with Red Fluorescent Protein (RFP) signals were merged automatically. Yellow light can be seen in the merged image, indicating co-localization of USP26 and KIF5B (Figure 2B).

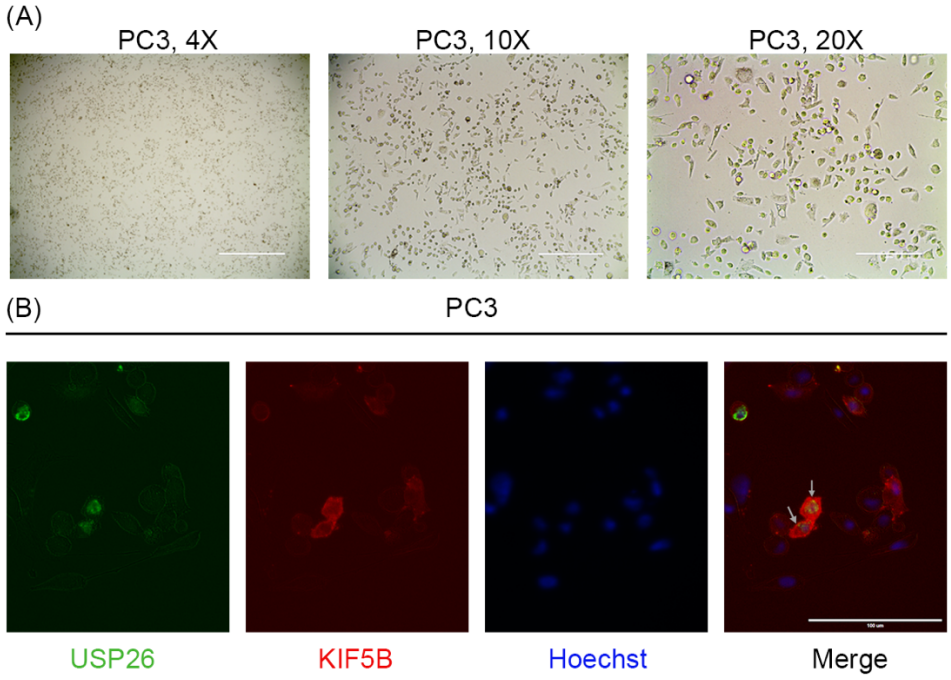

Figure 2. **USP26 co-localizes with KIF5B.** (A) The PC3 cells used for fluorescent imaging under bright field. (B) PC3 cells from (A) were co-transfected with eGFP-USP26 and mCh-KIF5B (truncated amino acids 1-555). After 24 hours of incubation, Hoechst 33342 (0.5% v/v, dissolved in the cell culture medium) was applied to the cell culture and incubated for 15 minutes. Live microscopy was performed to detect signals of GFP, RFP, and DAPI (equivalent to the Hoechst dye). Images from these three channels were automatically merged by the microscope software. The arrows in the merged image indicate the co-localization of USP26 and KIF5B (yellow pixels). The scale bar displays a length of 100 μm.

3.4 Knockdown of USP26 downregulates the protein but not the mRNA of KIF5B

To investigate the mechanism by which USP26 regulates KIF5B, qPCR and WB were used to analyze the expression of USP26 and KIF5B on mRNA and protein levels. According to the qPCR result, as the PC3 cell line was stably expressing the shUSP26 lentivector, USP26 was significantly knocked down (Figure 3A, $p<0.05$). On the other hand, no significant difference in KIF5B mRNA levels was detected between the stable cell line expressing shUSP26 and its control (Figure 3F). Meanwhile, SMAD7 was tested to validate the effectiveness of the USP26 knockdown since a previous study implies that the knockdown of USP26 downregulates Mothers Against Decapentaplegic Homolog 7 (SMAD7, Figure 3B) on the transcriptional level when the cells are not stimulated by TGF-β [18]. The result was consistent with the published literature. In addition, murine double minute 2 (MDM2, Figure 3C) and WD repeat and HMG-box DNA binding protein 1 (WDHD1) were also tested because MDM2 is a validated substrate of USP26, and MS screening indicates that WDHD1 is potentially a substrate of USP26 (Table 1) [19]. The qPCR results indicate that the knockdown of USP26 downregulates their mRNA levels. In addition, to investigate the controversial role of USP26-p53 interaction (unpublished work of Dr. Qiuyang Zhang's Lab) in PCa, the mRNA level of Tumor Protein p53 (encoded by *TP53*, which underwent a frame-shift mutation in the PC3 cell line) was also tested. The qPCR result indicates a positive correlation with USP26.

Interestingly, in the WB, the protein level of KIF5B was positively correlated with USP26 (Figure 3G). Thus, USP26 regulates the expression of KIF5B on the protein level but not on the mRNA level, implying that USP26 is very likely to act as a deubiquitinase (DUB) to regulate KIF5B. This downregulation of KIF5B is also confirmed in both intact

and castrated mice with *Usp26* conditionally knocked out in the prostate tissue (Figure 3H).

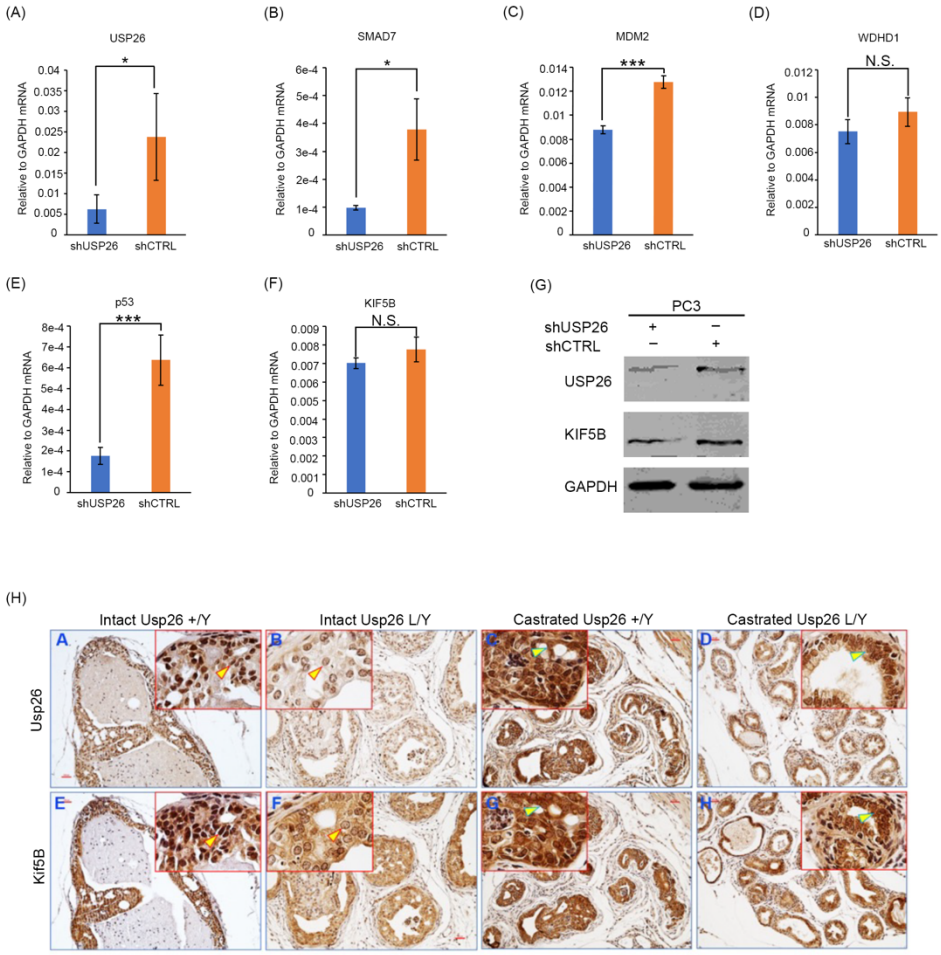

Figure 3. **Knockdown of USP26 downregulates the protein but not the mRNA level of KIF5B.** The term "shUSP26" stands for the PC3 stable cell line expressing shRNA of USP26, and the term "shCTRL" stands for "shRNA control," meaning the PC3 stable cell is stably expressing shRNA with a scrambled sequence. (A-F) The PC3 stable cell lines were seeded into 60 mm cell culture dishes and incubated for 24 hours, followed by qPCR. The Y-axis labels indicate the gene's mRNA level relative to *GAPDH*. The error bars stand

for the 95% confidence interval. The asterisks stand for significant differences (*: $p < 0.05$; **: $p < 0.01$; ***: $p < 0.001$ N.S: No Significance). (G) The PC3 stable cell lines were seeded into 60 mm cell culture dishes and incubated for 24 hours. The WB analysis shows the protein levels of USP26 and KIF5B. GAPDH is used as a loading control. (H) *Usp26* was conditionally knocked out in mice's prostate tissue using the Cre-LoxP system. *Usp26* was not knocked out when the genotype was "Usp26 +/Y." It was only knocked out when then genotype was "Usp26 L/Y."

3.5 USP26 cleaves K48-linked ubiquitin chains from KIF5B and inhibits its proteasomal degradation

To investigate the DUB activity of USP26 on KIF5B, HEK293T stable cell lines were established. In the cell line stably expressing shRNA of USP26, the protein level of both USP26 and KIF5B reduced compared to the one stably expressing scrambled shRNA (Figure 4A). A DUB activity test was performed using cell lines. The DUB activity test indicates that the ubiquitination of KIF5B is dramatically upregulated in the USP26-knockdown 293T cell line (Figure 4B).

Since ubiquitination is commonly associated with proteasomal degradation, the next step is to study the role of USP26 in KIF5B degradation. A CHX chase assay was performed as described in the chapter on Materials and Methods. It was readily visible that the degradation of KIF5B is more rapid when USP26 is knocked down (Figure 4C).

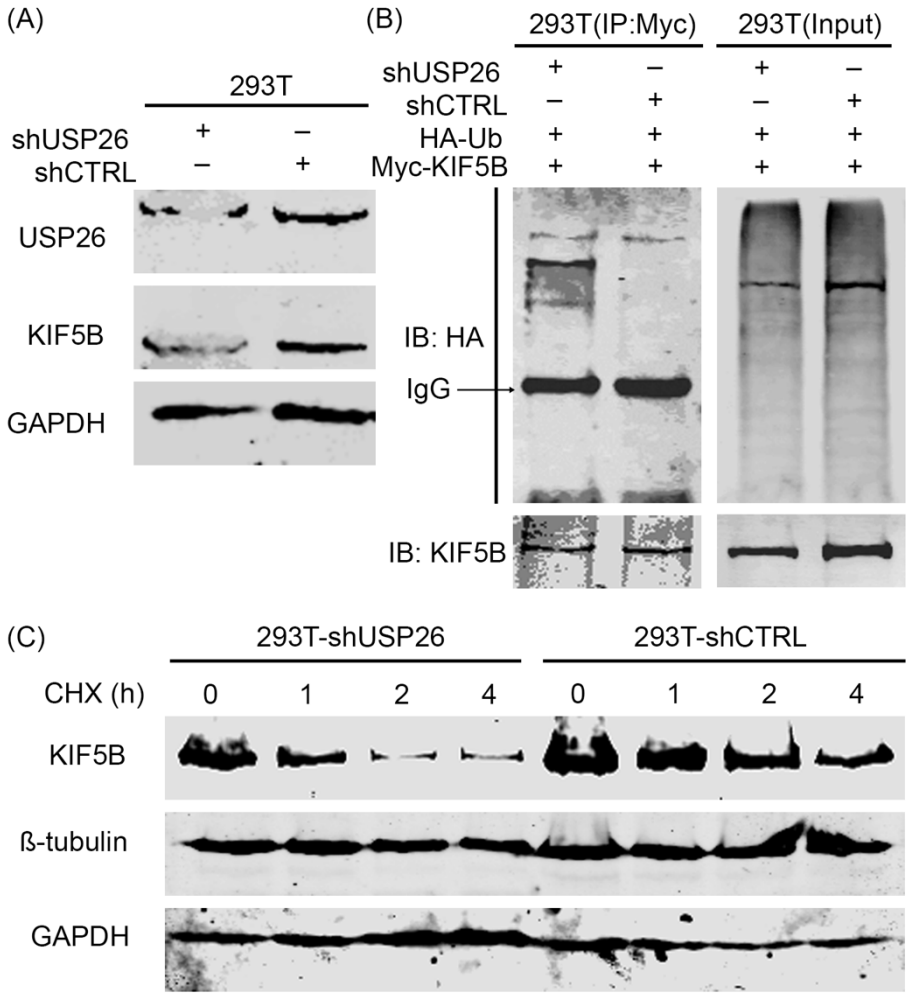

Figure 4. **Knockdown of USP26 upregulates ubiquitination and proteasomal degradation of KIF5B.** The term "shUSP26" stands for the 293T stable cell line expressing shRNA of USP26, and the term "shCTRL" stands for "shRNA control," meaning the 293T cell line is stably expressing shRNA with a scrambled sequence. (A) The 293T stable cell lines were seeded into 60 mm cell culture dishes and incubated for 24 hours. Proteins were extracted and proceeded with WB. (B) The 293T stable cell lines were seeded into 60 mm cell culture dishes and incubated for 24 hours. Each stable cell line was

co-transfected with KIF5B-Myc and HA-Ubiquitin (wildtype) and incubated for 24 hours. After four hours of treatment with 10 μM of MG-132, proteins were extracted from these samples and proceeded with Immunoprecipitation (IP), using an equal amount (1 μg) of Myc-tag antibody. The ubiquitination level of KIF5B was estimated with Western Blot (WB) analysis. "WT" stands for wildtype ubiquitin. (B) The 293T stable cell lines were seeded into 90 mm cell culture dishes and incubated for 24 hours. CHX (50 μg/ml) was applied to the cell cultures and incubated for 0, 1, 2, and 4 hours before proteins were extracted. The expression levels of KIF5B at these moments were estimated using WB analysis.

3.6 Knockdown of USP26 downregulates p-JNK and CLIP170

It has been established that KIF5B can promote microtubule dynamics by activating c-Jun N-terminus Kinase (JNK) [20, 21]. Given that USP26 regulates the proteasomal degradation of KIF5B, it is necessary to study whether USP26 can regulate the microtubule dynamics via the KIF5B-JNK axis. PC3 cells were transfected with the shUSP26 and scrambled shRNA lentiviral vector and proceeded with WB analysis. The phosphorylation level of JNK-2 was downregulated as the knockdown of USP26 downregulated KIF5B, while the total JNK-2 level remained constant (Figure 5A). In a preliminary study with the C4-2 cell line, a microtubule plus end tracking protein, Cytoplasmic Linker Protein of 170 kDa (CLIP170), was downregulated along with KIF5B as the cell was transfected with the shUSP26 lentiviral vector. Note that the WB analysis failed to detect the USP26 in this experiment (Figure 5B).

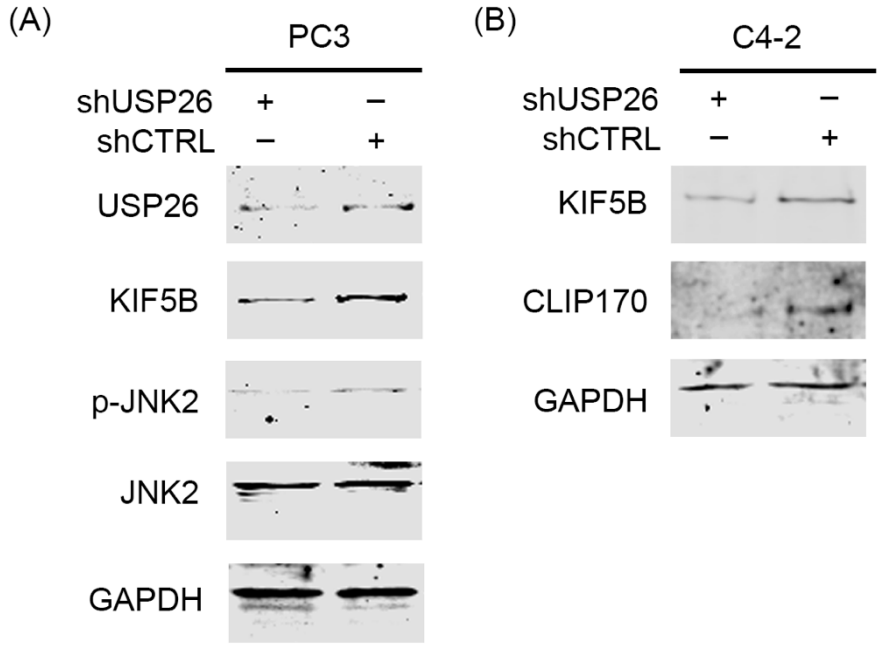

Figure 5. **Knockdown of USP26 downregulates p-JNK2 and CLIP170**. (A) PC3 cells were seeded in 60 mm culture dishes and incubated at 37ºC and 5% CO_2 for 24 hours. Cells from each culture dish were transfected with 6 μg of plasmids to express shRNA of human USP26 (shUSP26) or scrambled sequence as a control (shCTRL). Proteins were extracted and proceeded with Western Blot (WB) analysis. GAPDH was used as a loading control. (B) C4-2 cells were seeded in 60 mm culture dishes and incubated at 37ºC and 5% CO_2 for 24 hours. Cells from each culture dish were transfected with 6 μg of plasmids to express shRNA of human USP26 (shUSP26) or scrambled sequence as a control (shCTRL). Proteins were extracted and proceeded with WB analysis. GAPDH was used as a loading control.

4. Discussion

Although KIF5B is regulated by USP26, and knocking down USP26 can influence cellular behaviors such as colony formation and proliferation (Figure 1), the role of KIF5B in those cellular behaviors remains unclear. In addition, most studies related to KIF5B in cancer cells focus on the KIF5B-MET and cKIF5B-RET fusions [22, 23]. Not much research was done on KIF5B itself. Only one study identified KIF5B as a novel marker in pancreatic cancer [24]. Thus, further investigations are required, and it is necessary to eliminate the off-target effects of USP26 while studying the role of KIF5B.

USP26 mainly resides in the nucleus, and only a small portion is present in the cytoplasm to interact with KIF5B (Figure 2). Thus, a few points remain to be investigated in the future: (1) The phase of the cell cycle during which USP26 translocates to the cytoplasm; (2) The domain of USP26 that is essential for the translocation. The live fluorescent microscopy (Figure 2) also indicates that USP26 may interact with the truncated KIF5B (the motor domain). However, whether USP26 is a cargo of KIF5B remains unknown.

Based on current evidence, USP26 can regulate the KIF5B expression level by inhibiting its degradation using its DUB activity (Figure 4A). However, KIF5B is potentially subject to K63-linked or other atypical lysine-linked polyubiquitination [5]. USP26's DUB activity against these types of ubiquitinated KIF5B remains unclear.

It has been established that KIF5B depends on JNKs to regulate microtubule dynamics [20]. The study has validated that the phosphorylation level of JNK is positively associated with KIF5B expression level, and inhibition of JNK can make the microtubules less dynamic [20]. A review article also indicates that conventional kinesin's cargo, Jun-interacting Protein (JIP), serves as a scaffold where JNKs can be phosphorylated by the upstream Mitogen-activated Protein Kinase Kinases (MKKs) [21]. The phosphorylated (activated) JNKs then phosphorylate Microtubule-associated Proteins (MAPs) to facilitate microtubule growth [21]. Our study indicates that knockdown of USP26 may inhibit the phosphorylation of JNK-2 by downregulating KIF5B. Yet visual evidence of changes in the microtubule dynamics needs to be captured in future studies. Note that JNKs can also phosphorylate the Activating Protein 1 (AP-1) family members, including Jun and Fos proteins, which in turn promotes cell proliferation [25]. Since the knockdown of USP26 downregulates the phosphorylation level of JNK, this might explain USP26's ability to regulate cell proliferation (Figure 1A).

It is also noteworthy that CLIP170 was downregulated when USP26 was knocked down (Figure 5B). CLIP170 binds the plus end of microtubules and stabilizes them on the plus end [20, 21]. Changes in the level of CLIP170 indicate that USP26 may be participating in the regulation of microtubule dynamics, yet the exact mechanism remains to be explored. Besides the functions of a microtubule tracker and regulator, CLIP170 may also be an indicator of malignancy. It promotes the aggressiveness of breast cancer and is part of the signaling pathway that is responsible for the metastasis of salivary gland adenoid cystic carcinoma [26, 27]. These facts may partially explain the effects of USP26 knockdown on cellular behaviors (Figure 1).

5. Conclusion

Loss of function studies indicate that the knockdown of USP26 is associated with significantly less rapid proliferation even though one of its known substrates, AR, is absent in the PC3 cell line.

From MS screening, we identified KIF5B as a potential substrate of USP26. Live fluorescent microscopy reveals that USP26 co-localizes with KIF5B

Real-time qPCR, Western Blot analysis, and Immunohistochemistry on (mice's prostate tissue) indicate that USP26 positively regulates the protein but not the mRNA level of KIF5B in prostate cancer models regardless of castration resistance.

The DUB activity test indicates that the knockdown of USP26 causes the upregulation of KIF5B's ubiquitination level. The following CHX chase assay validates that the knockdown of USP26 promotes KIF5B's degradation rate.

In the end, our Western Blot analysis indicates that USP26 participates in the regulation of microtubule dynamics by stabilizing KIF5B (Figure 6).

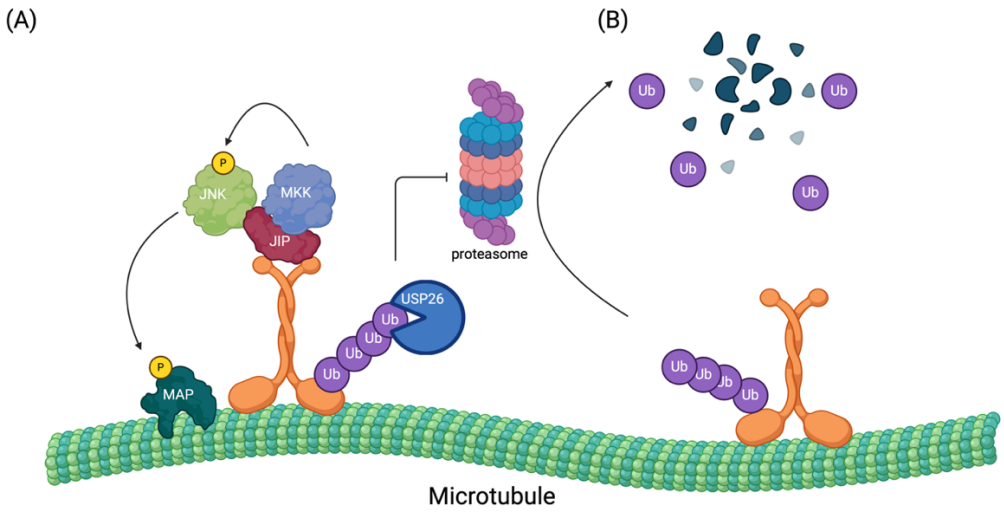

Figure 6. **Graphic Summary.** (A) When is abundant in the cell, it stabilizes KIF5B, allowing the recruitment of MKKs and JNKs through its cargo JIP (also a scaffold). JNK is phosphorylated by MKK, which in turn phosphorylates MAPs to regulate the microtubule dynamics. (B) When the USP26 level is low in the cell, KIF5B is subject to rapid proteasomal degradation. The subsequent events depicted in (A) are not going to happen. JNK, cJun N-terminus Kinase; JIP, JNK-Interacting Protein; MKK, Mitogen-activated Protein Kinase Kinase; MAP, Microtubule Associated Protein.

LIST OF REFERENCES

1. Wang, L., et al., *Prostate Cancer Incidence and Mortality: Global Status and Temporal Trends in 89 Countries From 2000 to 2019.* Front Public Health, 2022. **10**: p. 811044.

2. Xu, H., et al., *Preclinical Study Using ABT263 to Increase Enzalutamide Sensitivity to Suppress Prostate Cancer Progression Via Targeting BCL2/ROS/USP26 Axis Through Altering ARv7 Protein Degradation.* Cancers (Basel), 2020. **12**(4).

3. Hashemi, M., et al., *Paclitaxel and docetaxel resistance in prostate cancer: Molecular mechanisms and possible therapeutic strategies.* Biomed Pharmacother, 2023. **160**: p. 114392.

4. Carroll, E.C. and S. Marqusee, *Site-specific ubiquitination: Deconstructing the degradation tag.* Curr Opin Struct Biol, 2022. **73**: p. 102345.

5. Yang, Q., et al., *E3 ubiquitin ligases: styles, structures and functions.* Mol Biomed, 2021. **2**(1): p. 23.

6. Pohl, C. and I. Dikic, *Cellular quality control by the ubiquitin-proteasome system and autophagy.* Science, 2019. **366**(6467): p. 818-822.

7. van den Boomen, D.J.H., N. Volkmar, and P.J. Lehner, *Ubiquitin-mediated regulation of sterol homeostasis.* Curr Opin Cell Biol, 2020. **65**: p. 103-111.

8. Alsayyah, C., et al., *The regulation of mitochondrial homeostasis by the ubiquitin proteasome system.* Biochim Biophys Acta Bioenerg, 2020. **1861**(12): p. 148302.

9. Zhang, B. and R. Burke, *Copper homeostasis and the ubiquitin proteasome system.* Metallomics, 2023. **15**(3).

10. Zhou, Z., et al., *The Emerging Role of Deubiquitinases in Cell Death.* Biomolecules, 2022. **12**(12).

11. Lange, S.M., L.A. Armstrong, and Y. Kulathu, *Deubiquitinases: From mechanisms to their inhibition by small molecules.* Mol Cell, 2022. **82**(1): p. 15-29.

12. Chen, S., Y. Liu, and H. Zhou, *Advances in the Development Ubiquitin-Specific Peptidase (USP) Inhibitors.* Int J Mol Sci, 2021. **22**(9).

13. Li, Q.Y., et al., *The association between mutations in ubiquitin-specific protease 26 (USP26) and male infertility: a systematic review and meta-analysis.* Asian J Androl, 2022. **24**(4): p. 422-429.

14. Li, L., et al., *USP26 promotes esophageal squamous cell carcinoma metastasis through stabilizing Snail.* Cancer Lett, 2019. **448**: p. 52-60.

15. Tang, J., Y. Luo, and L. Xiao, *USP26 promotes anaplastic thyroid cancer progression by stabilizing TAZ.* Cell Death Dis, 2022. **13**(4): p. 326.

16. Dirac, A.M. and R. Bernards, *The deubiquitinating enzyme USP26 is a regulator of androgen receptor signaling.* Mol Cancer Res, 2010. **8**(6): p. 844-54.

17. Li, J., et al., *Membrane-associated androgen receptor (AR) potentiates its transcriptional activities by activating heat shock protein 27 (HSP27).* J Biol Chem, 2018. **293**(33): p. 12719-12729.

18. Kit Leng Lui, S., et al., *USP26 regulates TGF-beta signaling by deubiquitinating and stabilizing SMAD7.* EMBO Rep, 2017. **18**(5): p. 797-808.

19. Lahav-Baratz, S., et al., *The testis-specific USP26 is a deubiquitinating enzyme of the ubiquitin ligase Mdm2.* Biochem Biophys Res Commun, 2017. **482**(1): p. 106-111.

20. Daire, V., et al., *Kinesin-1 regulates microtubule dynamics via a c-Jun N-terminal kinase-dependent mechanism.* J Biol Chem, 2009. **284**(46): p. 31992-2001.

21. Benoit, B., A. Baillet, and C. Pous, *Cytoskeleton and Associated Proteins: Pleiotropic JNK Substrates and Regulators.* Int J Mol Sci, 2021. **22**(16).

22. Costa, E.S.M., et al., *KIF5B-MET fusion variant in non-small cell lung cancer.* Pulmonology, 2022. **28**(4): p. 315-316.

23. Song, M., S.H. Kim, and S.K. Yoon, *Cabozantinib for the treatment of non-small cell lung cancer with KIF5B-RET fusion. An example of swift repositioning.* Arch Pharm Res, 2015. **38**(12): p. 2120-3.

24. Charles Jacob, H.K., et al., *Identification of novel early pancreatic cancer biomarkers KIF5B and SFRP2 from "first contact" interactions in the tumor microenvironment.* J Exp Clin Cancer Res, 2022. **41**(1): p. 258.

25. Hammouda, M.B., et al., *The JNK Signaling Pathway in Inflammatory Skin Disorders and Cancer.* Cells, 2020. **9**(4).

26. Hu, Y., et al., *Tension of plus-end tracking protein Clip170 confers directionality and aggressiveness during breast cancer migration.* Cell Death Dis, 2022. **13**(10): p. 856.

27. Li, L., et al., *LIS1 interacts with CLIP170 to promote tumor growth and metastasis via the Cdc42 signaling pathway in salivary gland adenoid cystic carcinoma.* Int J Oncol, 2022. **61**(4).

TITLE PAGE

Literature Review: Nuclear Factor kappa B (NF-κB) Regulation in Human Cancers Mediated by Ubiquitin-Specific Proteases (USPs)

Keyi Shen[1], Qiuyang Zhang[1,2,3*]

[1]Department of Structural & Cellular Biology, Tulane University School of Medicine, New Orleans, LA, USA

[2]Tulane Center for Aging, Tulane University, New Orleans, LA, USA

[3]Tulane Cancer Center and Louisiana Cancer Research Center, Tulane University, New Orleans, LA, USA

[*]**Correspondence to:** Qiuyang Zhang, PhD, Department of Structural and Cellular Biology, Tulane University School of Medicine, 1430 Tulane Avenue SL-49, New Orleans, LA 70112, USA (e-mail: qzhang3@tulane.edu).

Running Title: USPs Regulate NF-κB Signaling in Human Cancers

Keywords: NF-κB, Human Cancer, Prostate Cancer, USPs

Correspondence:

Qiuyang Zhang, Ph.D.

Assistant Professor

Department of Structural & Cellular Biology

Tulane University School of Medicine

1430 Tulane Avenue, SL8649

New Orleans, LA 70112-2699, USA.

Office: 504-988-5527

Fax: 001 504 988 1687

E-mail: qzhang3@tulane.edu

Word Count: 5948

Number of figures: 2; tables: 2

Contributions: (I) Conception and design: Both authors; (II) Administrative support: Qiuyang Zhang; (III) Provision of study materials or patients: None; (IV) Collection and assembly of data: Keyi Shen; (V) Data analysis and interpretation: Both authors; (VI) Manuscript writing: Both authors; (VII) Final approval of manuscript: Both authors.

(This paper has been submitted to Annuals of Translational Medicine. It is currently under review.)

ABSTRACT

Background and Objective: The nuclear factor kappa B (NF-κB) consists of a group of transcription factors of which its dysregulation is responsible for diseases such as inflammation and cancer. Ubiquitin-specific proteases (USPs) are the most prominent group among the Deubiquitinases. Their functions include control of protein stability and regulation of signaling transduction. The association between NF-κB activity and human cancer progression is evident. Still, the role of USPs in the NF-κB regulation in human cancers, especially prostate cancer, is not well understood. This review discusses on the role of USP-mediated regulation of the canonical NF-κB signaling pathway in human cancers and provides a prospect of future studies in prostate cancers.

Methods: Within the biomedical literature database, PubMed, our review team searched for keywords including ubiquitin-specific protease (USP), NF-κB signaling pathway, and combinations of specific USPs (USP1, USP2, etc.) and the keyword NF-κB. After screening, only mechanistic studies and articles reporting the subsequent changes in cellular behaviors were included for full-text review.

Key Content and Findings: Most USPs function primarily as deubiquitinases (DUBs) to regulate the canonical NF-κB signaling pathway. The typical K48- and K63-linked DUB activities of USPs are the best understood. These USPs are positive and negative regulators

of the NF-κB activity. However, their DUB activities against polyubiquitin chains with atypical linkages have not yet been extensively studied. Furthermore, some USPs can regulate the canonical NF-κB signaling pathway via ubiquitin-independent mechanisms.

Conclusions: In the regulation of the canonical NF-κB pathway, the USPs function primarily as DUBs, but they also regulate the p65/p50 by ubiquitin-independent mechanisms. Generally, in human cancer models, USP-mediated elevation, and suppression of p65/p50 activity lead to more or less malignant cellular behaviors, respectively. Given the currently unbalanced focus on K48- and K63-linked DUB activities and the context-dependent function of USPs, future research of USP-mediated NF-κB regulation in human cancers should invest more in the DUB activities against the atypical polyubiquitin chains and test known mechanisms in different cancer models.

1. Introduction

1.1 Background

Cancer is one of the most lethal diseases in humans. In 2020, there were 1,414,259 new cases of prostate cancer and 375,304 related deaths reported globally, and age-standardized incidence and mortality rates were increasing in 65 and 19 countries, respectively [1]. There is an urgent need to improve understanding of the development and progression of prostate cancer and identify potential novel treatments for it. Examining signaling pathways widely conserved in different cancer models may provide insight into potential druggable targets. The canonical NF-κB signaling pathway is one of them. It promotes cell survival, proliferation, invasion, and migration in multiple cancers. Thus, the regulatory mechanisms of the canonical NF-κB signaling pathway may provide opportunities for the development of novel treatments. Regulation of signaling molecules is often actuated through post-translational modifications, including phosphorylation, ubiquitination, acetylation, and methylation. This review will focus on the role of ubiquitination and deubiquitination systems in the NF-κB activity regulatory mechanisms, especially USPs' role in regulating NF-κB signaling.

1.2 Rationale and Knowledge Gap

Firstly, although the role of Deubiquitinases (DUBs) such as tumor necrosis factor alpha-induced protein 3 (TNFAIP3, A20) and cylindromatosis lysine 63 deubiquitinase (CYLD) in DUB-mediated NF-κB regulation has been reviewed, a general understanding

of the functions of USPs (the largest family of DUBs) in the NF-κB regulation has not been established [2]. A literature review can provide a general understanding of the current knowledge in USP-mediated regulation of the canonical NF-κB signaling pathway in human cancers and potentially guide the future study of NF-κB regulation in certain cancers.

Secondly, Knowledge gaps exist between the conventional belief and novel findings in the ubiquitination and deubiquitination systems. Ubiquitin was discovered in the 1970s [3]. The linkage of polyubiquitin chains determines the function of the target protein. Traditionally, it is widely accepted that the lysine-48 (K48)-linked polyubiquitin chain leads to proteasomal degradation, and the K63-linked polyubiquitin chain serves as a scaffold for the recruitment of downstream signaling molecules (Figure 1) [4, 5]. These two typical linkages of polyubiquitin chains are the most extensively studied, but the remaining atypical polyubiquitin chains are not well understood. A literature review involving USP-mediated NF-κB regulation in human cancers can find out the size of this knowledge gap from the angle of the deubiquitination system in this specific area of cancer research and provide potential directions for future studies.

1.3 Objective

This manuscript is written following the Narrative Review checklist. This review aims to summarize the research progress on the NF-κB regulating mechanisms mediated by USPs in human cancers and their influences on cellular behaviors. Based on summarized regulatory mechanisms and the knowledge gaps identified during this process, this review will provide a prospect for future research on NF-κB regulation mediated by USPs in human cancers.

2. Methods

A preliminary search was conducted in the biomedical literature database PubMed. Keywords included ubiquitin-specific proteases (USP), NF-κB signaling pathways, and combinations of keywords such as "NF-κB" and specific USPs such as USP1, USP2, USP3, etc (Table 1). Results from the preliminary search were screened for full-text review. Only the ones with precise mechanisms and those demonstrating the influences of USP-mediated NF-κB regulation on cellular behaviors passed the screening (Table 1). During the full-text review, studies were excluded if the regulatory mechanisms involve proteins that are not ubiquitously expressed.

Table 1. The search strategy summary

Items	**Specification**
Date of Search	Dec. 1, 2023
Databases and other sources searched	PubMed
Search term used	Ubiquitin specific proteases, USP1, USP2, USP3, ..., USP53, NF-κB, cancer, and prostate cancer (Terms were used individually and in combinations).
Timeframe	2003 – 2023
Inclusion and exclusion criteria	Inclusion Criteria: 1. Original research articles must explain the mechanisms on the molecular level. 2. Regulatory Targets of USPs must be ubiquitously expressed. Exclusion Criteria: 1. The substrate of USPs is only expressed in limited types of cells or tissue.
Selection Process	The first author, Keyi Shen, conducted the selection independently. Consensus was achieved by discussion between the first author and corresponding author.
Any additional considerations, if applicable	N/A

N/A, Not Applicable

3. Key Content and Findings

3.1 Conventional Understanding and Novel Findings about Ubiquitination and Deubiquitination

Ubiquitin is a small protein consisting of 76 amino acids, equivalent to a molecular weight of approximately 8.5 kDa. Seven of these amino acids are lysine (K) residues that determine the linking pattern of polyubiquitin chains and functions of the ubiquitinated protein (Figure 1). It is conventionally accepted that K48-linked polyubiquitination is associated with proteasomal degradation, while K63-linked polyubiquitination is generally involved in signal transduction [4, 5]. Recent studies have unraveled the functions of some atypical polyubiquitin chains on the molecular level. Similar to K48, K11- and K29-linked polyubiquitination account for proteasomal degradation as well (Figure 1A) [6]. Besides its role in signaling transduction, K63-linked polyubiquitination is also associated with protein degradation via a proteasome-independent pathway during autophagy (both mechanisms are summarized in Figure 1) [6]. The K33-linked polyubiquitin chain is responsible for the separation of the signal transducer and activator of transcription 3 (STAT3) from DNA [6]. In other words, the K33-linked polyubiquitin chain can inhibit protein-DNA interaction. Besides the lysine-dependent polymerization, ubiquitin molecules can also be linked linearly (in an N-terminus-to-C-terminus manner) in the context of NF-κB regulation [7]. Ubiquitination requires three enzymes – E1 activating enzyme, E2 conjugating enzyme, and E3 ligase. The collaboration of E1, E2, and E3 enzymes facilitates the covalent bonding between ubiquitin and the target protein (Figure

1). On the other hand, the reverse of ubiquitination, which is deubiquitination, involves a class of enzymes named deubiquitinases (DUBs, Figure 1D).

A total of 102 DUBs in humans can be divided into two classes – cysteine (also known as thiol) proteases and metalloproteases [8]. Cysteine proteases consist of 6 superfamilies – the ubiquitin-specific proteases (USPs), the ovarian tumor (OTUs) superfamily, the Machado-Josephin domain (MJDs) superfamily, the ubiquitin C-terminal hydrolases (UCHs), the K48-specific MIU-containing novel DUBs (MINDYs), and the K63-specific Zinc finger with Ubiquitin fold modifier (UFM)1-specific peptidase domain protein (ZUSFP) [8]. The ubiquitin-specific proteases (USPs) make up the most prominent family of DUBs with over 60 members [9, 10]. They remove polyubiquitin chains from their substrates, including the proteins involved in the regulation of the canonical NF-κB signaling pathways.

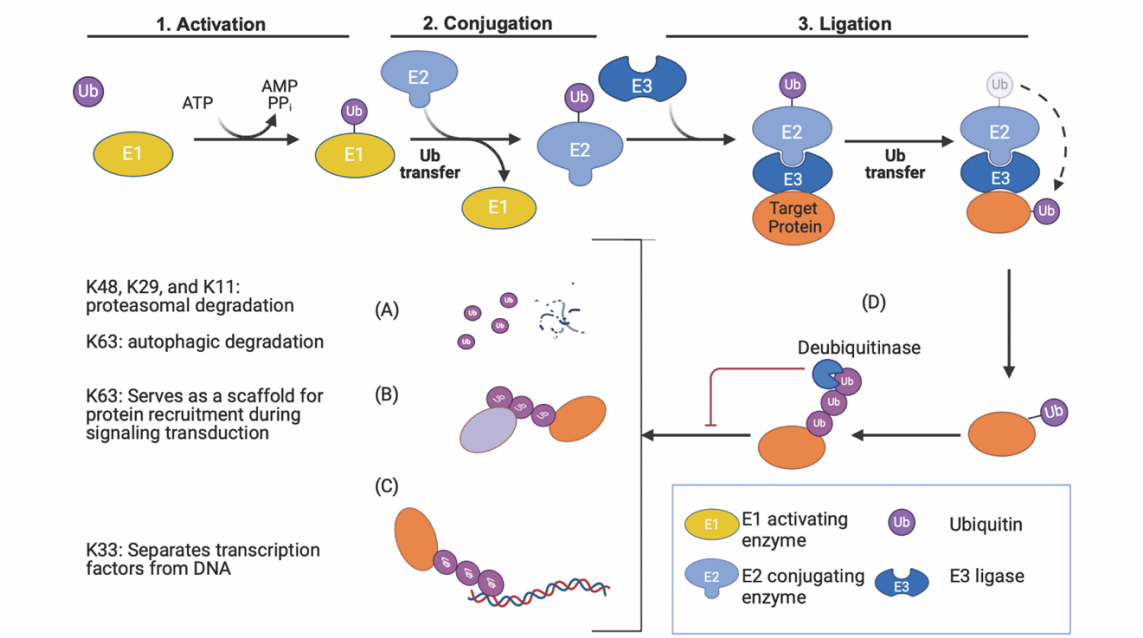

Figure 1. **Summary of Ubiquitination and Deubiquitination.** Ubiquitin is activated by the E1-activating enzyme, using 1 ATP. The activated ubiquitin is conjugated with the E2-

conjugating enzyme. Then, E3 ligase facilitates the transfer of ubiquitin from the E2-conjugating enzyme to the target protein. At this moment, the target protein is monoubiquitinated. If this process is repeated multiple times, the target protein will be polyubiquitinated and have a chain of many ubiquitin molecules. (A) If the polyubiquitin chain is linked by the lysine-48, 29, and 11 (K48, K29, and K11) residue in the ubiquitin, the polyubiquitinated protein will be recognized and digested by the proteasome. If the polyubiquitin chain is linked by the lysine-63 (K63) residue, it is subject to autophagic degradation. (B) If the polyubiquitin chain is linked by the lysine-63 (K63) residue in the ubiquitin, the polyubiquitinated protein will serve as a scaffold for protein recruitment during signaling transduction. (C) The K33-linked polyubiquitin chain can inhibit the protein-DNA interaction. (D) The target protein with a polyubiquitin chain can be recognized by DUBs. As a result, polyubiquitination can be reversed, and events described in (A-C) can be inhibited by the deubiquitinases (DUBs).

3.2 The Basics of NF-κB

NF-κB is a family of five transcription factors – NF-κB1 (p50/p105), NF-κB2 (p52/p100), p65 (RelA), c-Rel, and RelB, where p105 and p100 are precursors of p50 and p52 respectively [11]. In the canonical NF-κB pathway (Figure 2), the inactivated form of p65-p50 heterodimer is bound to the inhibitor of κB (IκB) in the cytoplasm. Upon phosphorylation by the IκB Kinase (IKK) complex, a complex consisting of IKKα, IKKβ, and NF-κB Essential Modulator (NEMO, or IKKγ), IκB is ubiquitinated and subject to proteasomal degradation. The degradation of IκB releases p65-p50 dimer, which is phosphorylated (on the p65 subunit) and translocated into the nucleus to activate the

transcription of target genes involved in inflammation and oncogenesis [11]. In the non-canonical pathway, the NF-κB inducing kinase (NIK) forms a complex with two IKKα subunits to phosphorylate the p100 subunit in the RelB/p100 heterodimer, inducing its cleavage (p100-p52 conversion) and activation [11]. This review will focus on the regulation of the canonical NF-κB pathway (p65/p50) by the USPs.

3.3 NF-κB in Human Cancer

Alterations of the canonical NF-κB signaling pathway are detected in multiple solid tumors, including pancreatic, lung, cervical, prostate, breast, and gastric carcinoma [12]. High levels of p65 are found in non-small cell lung carcinoma and breast cancer [13, 14]. IκB deficiency is detected in breast, colon, ovarian, pancreatic, bladder, prostate cancers, and melanoma. Constitutively active IKK is found in colorectal carcinomas [15].

3.4 Upstream Inducing Pathways are Subject to Regulation by USPs

Even though the NF-κB family exclusively consists of intracellular proteins, their activation is often induced by extracellular signals via surface receptors such as Tumor Necrosis Factor Receptor (TNFR), Toll-Like Receptor (TLR), and Interleukin (IL) 1 Receptor (IL-1R) (Figure 2). The signaling cascades following the activation of these surface receptors can usually be altered and, therefore, become regulatory sites for the activity of the canonical NF-κB signaling pathways [7, 16-18].

3.4.1 TNFR-Induced p65/p50 Activation is Subject to USP-mediated Regulation

TNFR can induce the activation of the canonical NF-κB signaling pathway from its upstream, and proteins in this upstream pathway are subject to regulation mediated by USPs. Upon stimulation of TNF-α (Figure 2A), TNFR1 recruits receptor interacting protein (RIP) 1 and TNF receptor associated factor (TRAF) 2 (an E3 ligase) to form a receptor complex using its tumor necrosis factor receptor type 1-associated DEATH domain (TRADD) domain [7, 16]. TRAF2 conjugates the K63-linked polyubiquitin chain to RIP1 and itself with the presence of Ubc13 and UeV1A (both are E2 conjugating enzymes) to recruit the transforming growth factor-*β*-activated kinase 1 (TAK1) complex (a heterotrimer of TAK1, Mitogen-activated protein kinase kinase kinase 7-interacting protein 1 (TAB1), and TAB2/3) and the IKK complex [7, 16]. The TRAF2-RIP1 complex recruits clAP1/2, a ubiquitin ligase and scaffold protein for the linear ubiquitin chain assembly complex (LUBAC), which later synthesizes a K63-linked or linear polyubiquitin chain that links to the TAB2/3 subunit in the TAK1 complex and the NEMO subunit in the IKK complex to recruit them [7, 16]. The recruited TAK1 complex undergoes autophosphorylation and activates the IKK complex by phosphorylation of IKKβ. The activated IKK complex phosphorylates IκB to induce its K48-linked polyubiquitination and proteasomal degradation [7, 16, 18]. Eventually, the degradation of IκB causes the release of p65/p50 dimer, which translocates into the nucleus and leads to subsequent transcriptional activities [7, 16, 18]. Meanwhile, IKK can also be activated in a TAK1-independent manner [19]. RIP1 in the receptor complex can interact with p62 to activate atypical Protein Kinase C (aPKCs), which in turn phosphorylates and activates the IKK complex [19].

In the TNFR-induced p65/p50 activation, the signaling cascades downstream of TRAF2 are shared by the TLR and IL-1R pathways (Figure 2B-2C), which is covered in upcoming sections of this review. Proteins unique to the TNFR pathway include TNFR, TRAF2, RIP1, and the aPKC. They can be regulatory sites for TNFR-induced NF-κB activity.

RIP1 can be a target for USP-mediated regulation. An *in vitro* study in cervical cancer cells shows that USP21 can remove K63-linked polyubiquitin chains from RIP1 (Figure 2A, Table 2). As a result, p65/p50 activation is inhibited [20].

Similar to RIP1, TRAF2 is another regulatory site specific to the TNFR-p65/p50 pathway. Although USP4, 19, and 31 all interact with TRAF2 in the TNFR-p65/p50 pathway, the outcomes are different (Figure 2A) [21-23]. A study in the pulmonary carcinoma model reveals that USP4 interacts with K63-linked TRAF2 and deubiquitates it to inhibit TNF-α-induced p65/p50 activation [22]. In this case, USP4-knockdown pulmonary carcinoma has a significantly higher migration rate than its control upon treatment of TNF-α [22]. This inhibitory mechanism was also discovered in a study of USP31 conducted in the HEK293T cell line [21]. On the other hand, a study in cardiac cells indicates that USP19 stabilizes TRAF2 by removing its K48-linked polyubiquitin chain [23]. In this case, the stabilized TRAF2 promotes the p65/p50 activation, which results in elevated cell viability [23].

The p62 protein is also a regulatory site specific to the TNFR-p65/p50 pathway (Figure 2A). It is reported that USP20 removes the K48-linked polyubiquitin chains on p62 to rescue it from proteasomal degradation [24]. Consequently, TNF-α-induced p65/p50 activity is promoted [24]. This study was conducted in a cervical cancer model and uncovered

that USP20-mediated p62 stabilization and subsequent upregulation of p65/p50 activity contribute to cancer cell survival [24].

3.4.2 IL-1R and TLR-induced p65/p50 Activation are Subject to USP-mediated Regulation

In a similar manner as TNFR, Interleukin-1 Receptor (IL-1R) and Toll-like Receptors (TLRs) share a pathways that induces activation of the IKK complex and, therefore, the activation of p65/p50 heterodimer in the canonical NF-κB signaling pathway (Figure 2B). This pathway provides opportunities for USPs to regulate the downstream p65/p50 activity indirectly. IL-1R is stimulated by IL-1, and the TLRs are stimulated by various ligands such as lipopolysaccharides (LPS) and viral DNA [17, 18, 25-30]. Upon stimulation, the receptors recruit Myeloid differentiation primary response 88 (MyD88), Toll-interacting protein (TOLLIP), IL-1 receptor associated kinase 1 (IRAK1), IRAK4, and TRAF6 to form a complex [16-18]. At this stage, IRAK1 undergoes autophosphorylation and phosphorylates IRAK4 to trigger the dissociation of the IRAK1-TRAF6 complex from the receptor complex [19]. Meanwhile, with the assistance of Ubc13 and Uev1A, TRAF6 undergoes K63-linked autoubiquitination and uses a K63-linked polyubiquitin chain to recruit the TAK1 complex via the TAB2/3 subunit and IKK complex via the NEMO subunit [18]. From this point and beyond, the IL-1R, TLRs, and TNFR share the same mechanism to activate the canonical NF-κB signaling pathway [7, 16-18]. For TLR-4, an extensively studied TLR, there is also a MyD88-independent pathway upstream of TRAF6 in addition to the MyD88-dependent pathway described above (Figure 2C). Upon stimulation of LPS trafficked by Cluster of Differentiation 14 (CD14), it uses TRIF [TIR (Toll/interleukin-1 receptor)

domain-containing adaptor protein inducing interferon beta; also known as TICAM-1 (TIR-containing adaptor molecule-1)] to recruit RIP1 and TRAF6 [16-18]. MyD88, TOLLIP, IRAK1/4, and TRAF6 are specific to the IL-1R/TLR-induced p65/p50 activating mechanism, and TRIF is a protein specific to TLR-4. All these proteins can be targets for indirect regulation of p65/p50 activation.

TRAF6 is shared by IL-1R and TLRs to induce p65/p50 activation, making it an effective regulatory site for mechanisms involving these receptors (Figure 2B-2C) [16, 18]. It is a target for USPs with proteasome-dependent and proteasome-independent DUB activities. Mechanistic studies demonstrate that USP2a, 3, 4, 10, 20, and 31 deactivate TRAF6 by removing the K63-linked polyubiquitin chain from it (Table 2 and Figure 2) [21, 22, 31-35]. Investigations on the cellular behaviors imply that the USP-mediated K63-linked deubiquitination of TRAF6 leads to suppressed malignant behaviors of cancer cells such as pulmonary carcinoma and HTLV-1 transformed T-cell leukemia [22, 33]. On the other hand, the proteasome-associated DUB activity of USPs stabilizes TRAF6 to promote NF-κB signaling. USP1, 4, 5, and 7 stabilize TRAF6 through their deubiquitinase activity [36-39]. USP4-mediated TRAF6 stabilization was studied in pancreatic cancer models (MIA PaCa-2 and AsPC-1) [38]. This study supports the idea that USP-mediated TRAF6 stabilization and subsequently upregulated NF-κB signaling are responsible for increased malignancy [38].

Usually, USPs stabilize proteins using deubiquitinase activity, which protects proteins from proteasomal degradation. Yet, there is an exception. In the case of viral infection, USP25 elevates the expression level of TRAF6 in a UPS-independent manner to promote NF-κB signaling [40].

3.4.4 Crosstalk Between PI3K-AKT and the Canonical NF-κB Pathway is Regulated by USPs

Surface receptors such as G-protein-coupled receptors (GPCRs) and Receptor Tyrosine Kinases (RTKs) can also activate p65/p50 dimer via an upstream inducing pathway – phosphoinositide 3-kinase (PI3K)-AKT axis (Figure 2D) [41-44]. Upon stimulation of hormones (via GPCR) or growth factors (via RTK), PI3K is activated to convert Phosphatidylinositol 4,5-Bisphosphate **(**PIP2) into Phosphatidylinositol 3,4,5-Trisphosphate (PIP3). Subsequently, PIP3 activates the pyruvate dehydrogenase kinase 1 (PDK1) and the mechanistic target of rapamycin (mTOR) complex 2 (mTORC2) to phosphorylate AKT at T308 and S473, respectively, to convert AKT into the active form, pAKT [42, 43]. The active pAKT can cause the activation of the NF-κB signaling pathway by phosphorylating IKKα [43]. On the other hand, the conversion from PIP2 to PIP3 is reversed by phosphatase and tensin homolog deleted on chromosome 10 (PTEN), a tumor suppressor protein [42-44]. Proteins specific to the crosstalk between PI3K/AKT and the canonical NF-κB signaling pathway include the surface receptor, PI3K, mTORC2, and PDK. They can be potential sites for indirect regulation of p65/p50 activation.

Epithelial Growth Factor (EGF) Receptor (EGFR, a type of RTK) and PI3K can be deubiquitinated and stabilized by USPs (Figure 2D). A mechanistic study in androgen-independent prostate cancer models (PC3 and DU145) unravels that USP8 catalyzes the deubiquitination of both EGFR and PI3K to stabilize them, which in turn activates IKKα to upregulate the p65/p50 activity [41]. Subsequently, upregulated p65/p50 activity results in an increase in N-cadherin and a decrease in E-cadherin (EMT marker), cleaved caspase 3, and cleaved caspase 9 (apoptosis markers) [41]. The *in vitro* functional study indicates that

USP8 is responsible for the inhibition of apoptosis, increase in cell proliferation and migration, and the development of docetaxel resistance of prostate cancer [41].

In contrast, USP13 reverses the effects of EGF-induced p65/p50 activity by interacting and stabilizing PTEN to suppress the p65/p50 activity (Figure 2D) [44]. The *in vitro* functional study reveals that USP13 knockdown exacerbates the colony formation, proliferation, invasion, and migration of bladder cancer cells, which can be reversed by re-expression of PTEN [44]. The *in vivo* rescue experiments also indicate that re-expression of USP13 or PTEN can partially restore tumor growth due to PTEN or USP13 knockout, respectively [44].

3.5 Signaling Cascades Shared by Upstream Inducing Pathways are Regulated by USPs

The regulatory mechanisms presented above are unique to each upstream inducing pathway. These pathways share some signaling cascades that eventually converge into the IKK-p65/p50 axis (Figure 2E-2F), and their signaling molecules are potentially USP's substrates. The TNFR, IL-1R, and TLR pathways share everything downstream of the TRAF proteins (TRAF2 and TRAF6, Figure 2A-2C), and the PI3K/AKT pathway shares the IKK-p65/p50 axis with all three of them (Figure 2D) [7, 16-18, 42, 43].

3.5.1 The TAK1 Complex is Regulated by USPs

Shared by the TNFR, IL-1R, and TLR pathways, the TAK1 complex is a regulatory site where USPs can indirectly control the p65/p50 activity [7, 16-18]. Given the recruiting and activating mechanisms (K63-linked polyubiquitin chains), the K63-linked DUB activity of

USPs can inhibit the TAK1 activity and subsequent p65/p50 activation. Mechanistic studies demonstrate that USP4, 18, and 19 dissociate the K63-linked polyubiquitin chain from the TAK1 subunit (Table 2 and Figure 2A-2C) [45-49]. In the study of USP19-mediated regulation p65/p50 activity, evidence also supports that USP19 cleaves off the K27-linked polyubiquitin chain as well, and the TAK1-TAB2/3 binding was disrupted [49]. A different study involving various in vitro cancer models provides evidence that USP18-mediated p65/p50 inhibition causes inhibited proliferation and increased apoptosis in leukemia, multiple myeloma, B-cell lymphoma, and cervical cancer cells [50].

Another TAK1-regulating protein is USP38 (Table 2). However, USP38-mediated TAK1 regulation does not involve the DUB activity of USP38. A study on USP38-mediated post-myocardial-infarction (post-MI) inflammation reveals that USP38 physically interacts with TAK1 and the conditional knockout of USP38 in mouse heart leads to a decrease in the phosphorylation level of TAK1 (pTAK1) and subsequent decrease in p65 activation [51]. Meanwhile, the TAK1 (native protein, not phosphorylated) level remains constant [51].

As a building block and the scaffold for recruitment of the entire functional complex, the expression level of the TAB2/3 subunit can also influence the TAK1 activity and the downstream p65/p50 activity. Thus, stabilizing TAB2/3 by USP using DUB activities associated with proteasomal degradation is another feasible option to potentiate the p65/p50 activity. A mechanistic study conducted in the HEK293T cell line reveals that USP15 stabilizes the TAB2 and TAB3 subunits of the TAK1 complex (Table 2) [52]. USP15 uses its K48-linked DUB activity to rescue TAB2 from proteasomal degradation (Figure 2A-2C), and USP15 also stabilizes TAB2 in a ubiquitin-independent mechanism – it inhibits the lysosomal degradation of TAB2 [52]. On the other hand, USP15 stabilizes TAB3

without using its DUB activity at all. Instead, it inhibits NBR1 (Neighbor of BRCA1 gene 1, a selective autophagy receptor) -mediated autophagic degradation of TAB3 [52].

3.5.2 NEMO is Regulated by USPs

Similar to the TAK1 complex, the IKK complex is also recruited to the surface receptors (TNFR, IL-1R, and TLRs) via a K63-linked polyubiquitin chain attached to its regulatory subunit – NEMO. Given this fact, it is potentially another regulatory site where USPs can indirectly control the p65/p50 activity. Studies indicate that the ubiquitination of the NEMO subunit is associated with both proteasomal degradation and signal transduction (Table 2) [35, 45, 53-55]. USP7 and USP10 remove the K63-linked polyubiquitin chain from NEMO to deactivate the IKK complex, resulting in the downregulation of p65/p50 activity (Figure 2A-2C) [35, 53]. USP18 is essentially the same in terms of function but slightly different in terms of mechanism. Instead of cleaving off the K63-linked polyubiquitin chain, it physically shields NEMO from K63-linked polyubiquitination [45]. Besides the K63-linked polyubiquitin chain, USP10 also removes linear polyubiquitin chains from the NEMO subunit in the IKK complex [54]. Removing the linear polyubiquitin chains from NEMO downregulates the p65/p50 activity to promote apoptosis *in vitro* and *in vivo* [54]. In addition, USP10-mediated deubiquitination of NEMO inhibits NEMO degradation and promotes p65/p50 activity in human leukemia monocytes and mouse macrophages [55].

3.6 The Common IKK-p65/p50 Axis is Regulated by USPs

Unlike the NEMO subunit, the IKKα and IKKβ subunits are involved in all four NF-κB inducing mechanisms described above (Figure 2). These two subunits are where all

those inducing pathways converge into the canonical NF-κB signaling pathway. Proteins in this common IKK-p65/p50 axis are subject to regulation mediated by USPs.

3.6.1 IKKβ is Regulated by USP3

As described in Table 2, it has been reported that ubiquitination of IKKβ is associated with proteasomal degradation [56]. USP3 can remove the polyubiquitin chain from IKKβ to stabilize it [56]. As a result, NF-κB activity is upregulated, and promoted tumor growth is detected in nasopharyngeal carcinoma [56].

3.6.2 The Expression Level of IκB is Altered by USPs by Various Means

The IκB-p65/p50 complex is immediately downstream of the IKK complex described above, and its degradation is induced by IKK-mediated phosphorylation, making it another effective regulatory site where USPs can function as DUBs (Figure 2E) [16, 18]. Deubiquitination of IκB can result in the stabilization of IκB and subsequent inhibition of p65/p50 activity. As summarized in Table 2, USP11, 15, 34, 39, and 53 interact with IκB-α and function as its DUBs to inhibit the degradation, and the USP-mediated IκB stabilization leads to the downregulation of p65/p50 activity [57-61]. The study of USP34-mediated IκB-α stabilization was conducted in immortalized mouse macrophages, where cell differentiation was inhibited [59]. In the study of USP53-mediated IκB stabilization, researchers found that USP53 inhibits the proliferation, invasion, and migration of renal cancer cells *in vitro* and *in vivo* [61].

It is widely agreed that deubiquitination of IκB leads to its stabilization and subsequent inhibition of p65/p50 activity. This is not necessarily true with USP14-IκB interaction (Table 2). A mechanistic study of IL-1β-induced NF-κB activity in human chondrocytes demonstrated that the p65 phosphorylation is positively correlated with USP14 despite USP14's DUB activity upon IκB-α [62]. A study on USP14-mediated NF-κB activation in endometrial carcinoma also confirms this result with a more readily visible negative correlation between the expression levels of USP14 and IκB-α [63]. The USP14-mediated p65/p50 activation inhibits apoptosis and increases malignant behaviors such as migration, invasion, and epithelial-to-mesenchymal transition (EMT) of endometrial carcinoma *in vivo* and *ex vivo* [63].

3.6.3 USPs Interact with p65 and Regulate p65 Activity

Upon release from IκB, the p65/p50 heterodimer is facing its destination – the nucleus (Figure 2F). The p65 subunit at this stage functions as a regulatory site for the canonical NF-κB signaling pathway. Deubiquitination of p65 by USP7, 15, and 48 can stabilize p65 and upregulate the NF-κB activity (Table 2) [64-66]. USP15 in multiple myeloma models accounts for inhibited apoptosis of cancer cells [65].

It is essential to clarify that USP48 specifically stabilizes nuclear p65 in HeLa and HEK293 cells when it is associated with COP9 signalosome (CSN), and USP48 preferably trims the K48-linked polyubiquitin chain instead of completely removing it [66]. Another study on USP48-mediated p65/p50 regulation conducted in retinal pigment epithelial cells unveils that knockdown of USP48 causes destabilization of both cytoplasmic and nuclear p65 and downregulates NF-κB activity despite the interaction between USP48 and p65 [67].

Another mechanism of USP-mediated p65 regulation is to induce its phosphorylation. The p65 phosphorylation requires USP6 to physically interact with both IKKα and IKKβ subunits in the IKK complex [68]. Results from xenografts support the idea that USP6-mediated p65 phosphorylation is associated with tumorigenesis *in vivo* [68].

3.7 Uncommon Regulatory Mechanisms

3.7.1 The p65/p50 Activity is Inhibited by USP35-mediated ABIN2 Stabilization

A20-binding Inhibitor of NF-κB 2 (ABIN2) is not a part of the NF-κB signaling pathway. Instead, it negatively regulates TNF-induced NF-κB signaling by competing with RIP1 for the NEMO subunit in the IKK complex [69]. Thus, USPs that function as DUBs of ABIN2 can stabilize it and inhibit the NF-κB activity. A study involving multiple cancer models revealed that USP35 inhibits TNF-α-induced NF-κB signaling by stabilizing ABIN2 with DUB activity [70]. The NF-κB inhibition through USP35-ABIN2 interaction leads to the inhibition of cancer cell proliferation in non-small cell lung carcinoma, cervical cancer, and prostate adenocarcinoma [70]. *In vivo* experiments also indicate that the USP35 inhibits tumor formation [70].

3.7.2 Phosphorylation of p65 is Induced by USP6

Although most USPs function as DUBs in NF-κB regulation, existing studies have identified a few exceptions. In addition to the ubiquitin-independent mechanisms of USP14 and USP25 mentioned above, USP6 can also regulate the NF-κB activity with a ubiquitin-independent method (Table 2). Despite its physical interaction with IKKα and IKKβ, USP6 does not influence the IκB expression level, which is immediately downstream of and

regulated by the IKK complex [68]. Instead, USP6 promotes phosphorylation of p65 with the presence of both IKKα and IKKβ. Knockdown of either subunit will result in a lower level of p65 in the nucleus [68]. Mice allografts stably expressing USP6 and its vector demonstrate that USP6-mediated NF-κB upregulation promotes tumorigenesis and tumor vascularization [68].

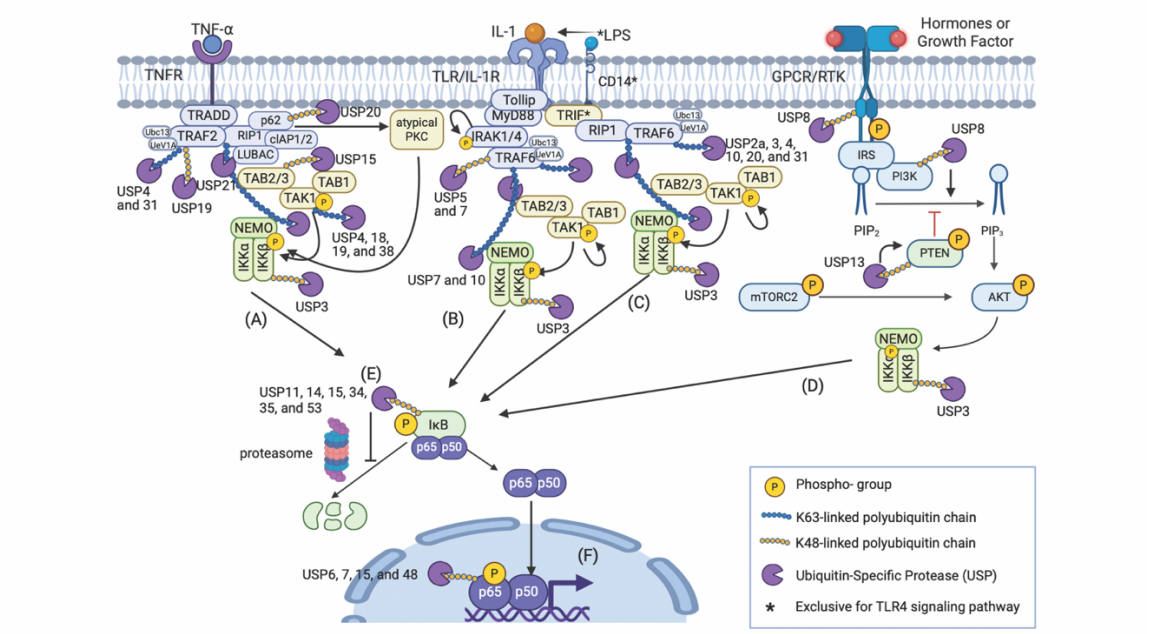

Figure 2. **USPs function as Deubiquitinases in the regulation of the TNFR-, TLR-, IL-1R-, and PI3K/AKT-induced p65/p50 activity.** (A) During the TNFR-induced p65/p50 activation, USPs can remove K63-linked polyubiquitin chains from TRAF2, RIP1, TAK1, and NEMO. They can also remove K48-linked polyubiquitin chains from p62, TAB2/3, and IKKβ. (B, C) Everything from and downstream of TRAF proteins during IL-1R- and TLR-induced p65/p50 activation are shared with the TNFR-induced pathway depicted in (A). The asterisk (*) in (C) indicates the labeled molecules belong to the TLR-4 pathway exclusively. (D) As an example for RTKs, during the EGFR-induced p65/p50 activation, USPs remove K48-linked polyubiquitin chains from the surface receptor (EGFR), PI3K,

and PTEN to regulate the p65/p50. Note that the stabilization of PI3K and PTEN will result in opposite effects on p65/p50 activity. (E) IκB is phosphorylated by the IKK complex. Phosphorylated IκB is conjugated with a K48-linked polyubiquitin chain and is subject to proteasomal degradation. USPs can stabilize IκB by removing this polyubiquitin chain. (F) Nuclear p65 can be conjugated with K48-linked polyubiquitin chains. This process can be reversed by the USPs listed above.

Table 2. The summary of USP-mediated NF-κB regulation

Target	NF-κB Activating Mechanism	Ubiquitin Chain Linkage	Regulating USPs	Effects on the Target	Effects on NF-κB activity	Effects on Cellular Behaviors	Cell/Tissue Types	Reference
RIP1	TNFR activation	K63	USP21	deactivated	negative	N/A	cervical cancer	20
TRAF2	TNFR activation	K63	USP31	deactivated	negative	N/A	Immortalized embryonic kidney cells	21
TRAF2	TNFR activation	K63	USP4	deactivated	negative	inhibited cell migration -increased cell viability - protection against mitochondrial dysfunction contribution to cell survival	pulmonary carcinoma	22
TRAF2	TNFR activation	K48	USP19	stabilized	positive		mouse cardiac cells	23
p62	TNFR activation	K48	USP20	stabilized	positive		cervical cancer	24
TRAF6	TRAF6 activation	K63	USP31	deactivated	negative	N/A	Immortalized embryonic kidney cells	21
TRAF6	TNFR activation	K63	USP4	deactivated	negative	inhibited cell migration	pulmonary carcinoma	22
TRAF6	viral infection	K63	USP2a	deactivated	negative	N/A	colorectal carcinoma	31
TRAF6	IL-1R activation	K63	USP3	deactivated	negative	inhibited apoptosis	chondrocytes	32
TRAF6	-HTLV-1 infection -IL-1R activation	K63	USP20	deactivated	negative	inhibited oncogenesis	HTLV-1 transformed cells (T-cell Leukemia)	33

TRAF6	IL-1R activation	K63	USP20	deactivated	negative	inhibited cell growth and proliferation	smooth muscle cells	34
TRAF6	Genotoxic Stress	K63	USP10	deactivated	negative	N/A	Immortalized embryonic kidney cells	35
TRAF6	N/A	N/A	USP1	stabilized	positive	inhibited pyroptosis	osteoblasts	39
TRAF6	TNFR activation	N/A	USP4	stabilized	positive	increased malignancy	pancreatic cancer	38
TRAF6	N/A	K48	USP5	stabilized	positive	increased expression of pro-inflammatory cytokine	Rheumatoid Arthritis-fibroblast-like synoviocytes	36
TRAF6	LPS-TLR4 interaction	K48	USP7	stabilized	positive	increased inflammation	immortalized mouse macrophages	37
TRAF6	viral infection	N/A	USP25	stabilized (by a ubiquitin-independent mechanism)	positive	increased expression of pro-inflammatory cytokine	mouse lung fibroblasts, plasmacytoid dendritic cells, and bone marrow derived dendritic cells	40
EGFR & PI3K	-EGFR activation - PI3K/AKT	N/A	USP8	stabilized	positive	cancer cell growth, proliferation, metastasis, and docetaxel resistance	androgen-independent prostate cancer	41
PTEN	PI3K/AKT	N/A	USP13	stabilized	negative	inhibited proliferation and metastasis	bladder cancer	44
TAK1	N/A	K63	USP18	deactivated	negative	N/A	immortalized embryonic kidney cells, cervical cancer cells, leukemia monocytes	45
TAK1	TNFR activation	K63	USP4	deactivated	negative	N/A	cervical cancer	46
TAK1	Doxorubicin	K63	USP4	deactivated	negative	N/A	cervical cancer, immortalized embryonic kidney cell, and mouse embryonic fibroblast	47

TAK1	-LPS-TLR4 interaction -CpG-TLR9 interaction	K63	USP18	deactivated	negative	inhibited expression of proinflam matory cytokines	mice model	48
TAK1	-TNFR activation -IL-1R activation	-K63 -K27	USP19	- deactivated - interaction with TAB2/3 is disrupted	negative	inhibited expression of proinflam matory cytokines	embryonic kidney cells	49
TAK1	N/A	N/A	USP18	N/A	negative	inhibited proliferati on and increase apoptosis	leukemia, multiple myeloma, B-cell lymphoma, and cervical cancer cells	50
TAK1	N/A	N/A	USP38	elevated phosphorylati on level stabilized (with both ubiquitin-dependent and ubiquitin-independent mechanisms)	positive	promoted post-myocardia l-infarction inflammat ion	mouse heart	51
TAB2	-TNFR activation -IL-1R activation	K48	USP15	stabilized (by inhibiting NBR1-induced autophagic degradation)	positive	N/A	Immortalized embryonic kidney cells	52
TAB3	–TNFR activation –IL-1R activation	N/A	USP15		positive	N/A	Immortalized embryonic kidney cells	52
NEMO	Genotoxic Stress	K63	USP10	deactivated	negative	N/A	Immortalized embryonic kidney cells	35
NEMO	N/A	N/A	USP18	deactivated (physically shielded from K63-linked poly-ubiquitination)	negative	N/A	immortalized embryonic kidney cells, cervical cancer cells, leukemia monocytes	45
NEMO	N/A	K63	USP7	deactivated	negative	N/A	colorectal carcinoma	53
NEMO	Genotoxic Stress	linear	USP10	deactivated	negative	promoted apoptosis	Immortalized embryonic kidney cells and mouse intestine tissue	54

NEMO	LPS-TLR4 interaction	N/A	USP10	stabilized	positive	promoted inflammatory response	leukemia monocytes and mouse macrophages	55
IKK-β	TNFR activation	N/A	USP3	stabilized	positive	promoted tumor growth	nasopharyngeal carcinoma	56
IκB-α	TNFR activation	K48	USP11	stabilized	negative	N/A	Immortalized embryonic kidney cells	57
IκB-α	TNFR activation	N/A	USP15	stabilized	negative	N/A	cervical cancer	58
IκB-α	N/A	N/A	USP34	stabilized	negative	inhibited differentiation	immortalized mouse macrophages	59
IκB-α	LPS-TLR4 interaction	K48	USP39	stabilized	negative	inhibited secretion of proinflammatory cytokines	leukemia monocytes	60
IκB-α	N/A	N/A	USP53	stabilized	negative	inhibited cell proliferation, invasion and migration	renal cancer cells	61
IκB-α	IL-1R activation	N/A	USP14	USP14 interacts with and deubiquitinates IκB-α, but suppresses its expression level	positive	inhibited differentiation -inhibited apoptosis -promoted EMT, colony formation, invasion, and metastasis	chondrocytes	62
IκB-α	N/A	N/A	USP14	USP14 interacts with and deubiquitinates IκB-α, but suppresses its expression level	positive	upregulated transcription	endometrial carcinoma	63
p65	N/A	N/A	USP7	stabilized	positive	inhibited apoptosis	immortalized mouse macrophages	64
p65	N/A	N/A	USP15	stabilized	positive	N/A	multiple myeloma	65
p65	TNFR activation -basal NF-κB activity -TNFR activation	K48	USP48	stabilized	positive	N/A	cervical cancer and embryonic kidney cells	66
p65		N/A	USP48	destabilized (via unknown mechanism)	negative	N/A	retinal pigment epithelial cells	67

p65	N/A	N/A	USP6	increased phosphorylation (with the presence of IKKα and IKKβ)	positive	promoted tumorigenesis inhibited cell proliferation (*in vitro*) and tumor formation (*in vivo*)	cervical cancer, mouse osteoblasts, and mouse embryonic fibroblasts non-small cell lung carcinoma and androgen-sensitive prostate adenocarcinoma	68
ABIN2	TNFR activation	N/A	USP35	stabilized	negative			70

NF-κB, Nuclear Factor kappa B; RIP1, Receptor Interacting Protein 1; TNF, Tumor Necrosis Factor; TNFR, Tumor Necrosis Factor Receptor; USP, Ubiquitin-Specific Protease; K63, lysine-63 residue (linked polyubiquitin chain); K48, lysine-48 residue (linked polyubiquitin chain); K27, lysine-27 residue (linked polyubiquitin chain); N/A, Not Applicable; TRAF, Tumor necrosis factor Receptor–Associated Factor; IL-1β, Interleukin-1β (isoform); IL-1R, Interleukin-1 Receptor; LPS, lipopolysaccharide; TLR, Toll-like Receptors; EGFR, Epithelial Growth Factor Receptor; PI3K, Phosphoinositide 3-Kinase; PTEN, Phosphatase and Tensin homolog deleted on chromosome 10; AKT, Ak Stain Transforming; TAK1, Transforming Growth Factor (TGF)-β-Activated Kinase 1; TAB, TAK1-Binding Protein; IκB-α, NF-κB Inhibitor α (isoform); IKK, IκB Kinase; NEMO, NF-κB Essential Modulator; ABIN, A20-Binding Inhibitor of NF-κB.

3.8 Discussion

3.8.1 Known Mechanisms and Missing Parts

In most studies summarized in Table 2, USPs primarily function as deubiquitinases (DUBs) to regulate the canonical NF-κB signaling pathway by removing polyubiquitin chains from signaling molecules in the TNFR-, TLR-, IL-1R-, and PI3K/AKT-induced canonical NF-κB pathway (Figure 2). The K48-linked DUB activity of USPs usually inhibits proteasomal degradation and stabilizes the target proteins, and K63-linked DUB activity usually downregulates signal transduction. K48-linked deubiquitination and stabilization of NF-κB's positive regulators, including TRAF proteins, TAK1, IKKα, IKKβ, and p65, lead to upregulation of p65/p50 activity. In contrast, stabilizing the negative regulators, including IκB-α and PTEN, can downregulate the p65/p50 activity. K63-linked deubiquitination and deactivation of NF-κB's positive regulators also downregulate the p65/p50 activity. TRAF proteins, TAK1, and NEMO undergo K63-linked deubiquitination

by USPs to inhibit NF-κB activation. These mechanisms are validated by studies conducted in different cancer models with different USPs. Thus, the existing studies have already covered USPs' function as DUBs in protein degradation and signaling transduction. Nevertheless, there are more problems that need to be addressed.

Firstly, it is essential to point out that USP-mediated p65/p50 regulation is context-dependent. Different proteins or the same proteins with different polyubiquitin chains can be the substrates of identical USPs. Thus, USPs have multifaced roles in the regulation of the canonical NF-κB pathway. USP4 sets up a good example. Studies demonstrate that USP4's substrates include TAK1, TRAF2, and TRAF6 (Table 2) [22, 38, 46, 47]. USP4 can detach the K63-linked polyubiquitin chains from all these proteins to downregulate the p65/p50 activity in multiple cell lines and inhibit cell migration of pulmonary carcinoma [22, 46, 47]. It can also stabilize TRAF6 by deubiquitination, promoting p65/p50 activity and malignant cellular behaviors in the pancreatic cancer cell lines [38]. In other words, despite the widely conserved regulatory mechanisms on the molecular level, the comprehensive effects of USP-mediated p65/p50 regulation on cellular behaviors depend on the context (for instance, the cell line or type of cancer). Thus, it is necessary to investigate the influence of USP-mediated NF-κB regulation individually in different cancer models.

Secondly, most of the mechanistic studies focus on the DUB activities against K48- and K63-linked polyubiquitin chains, and novel findings beyond the scope of these typical polyubiquitin chains are very limited. Only K27-linked polyubiquitinated TAK1 and linearly polyubiquitinated NEMO have been studied in USP-mediated p65/p50 regulation [49, 54]. K11- and K29-linked polyubiquitin chains are also associated with proteasomal degradation, and K63-linked polyubiquitin chains are responsible for autophagic

degradation (Figure 1). Many studies involving protein degradation in the p65/p50 regulation did not specify the linkage of the polyubiquitin chain (denoted by "N/A" in Table 2), leaving an unneglectable space for further investigation.

Thirdly, no USPs with K63-linked DUB activity have been identified as regulators of the TAB2/3 subunit in the TAK1 complex. Among the published studies, the only TAB2/3-regulating USP is USP15, and it only inhibits the degradation of TAB2 by K48-linked DUB activity (Table 2). Furthermore, USP15 more often regulates the degradation of TAB2 and TAB3 via ubiquitin-independent mechanisms. Given the fact that K63-linked polyubiquitination of TAB2/3 subunit is essential for TAK1 activation, this potential regulatory site deserves further investigation by screening USPs with K63-linked DUB activity.

Similar to TAB2/3, RIP1's activity relies on the K63-linked polyubiquitin chain, and it is essential for TNFR-induced p65/p50 activation. Existing evidence only supports that the K48-linked DUB activity of USP21 inhibits the proteasomal degradation of RIP1 [20]. None of the studies have identified a USP with K63-linked DUB activity against it, leaving a broad area for future research.

Another problem is the rarity of studies complicated with the lack of data on USP-mediated ubiquitin-independent regulatory mechanisms. It is also practical for the canonical NF-κB pathway to be regulated by the USPs in a ubiquitin-independent manner. Existing studies demonstrate that USP14 suppresses the expression level of IκB-α despite its ability to interact with and deubiquitinate IκB-α (Table 2) [62, 63]. This paradoxical result implies that there must be a ubiquitin-independent mechanism by which the USP14 regulates the IκB-α, and this mechanism must override the stabilizing effect of USP14's

DUB activity upon IκB-α. USP25 also promotes the RNA virus-induced p65/p50 activity by stabilizing TRAF6 through a ubiquitin-independent mechanism. Despite the physical interaction between USP25 and TRAF6, Western Blot analysis indicates that USP25 has neither K48- nor K63-linked DUB activity against TRAF6 [40]. However, USP25-positive cells maintain a higher level of TRAF6 and p-IκB-α [40]. USP6 is also a ubiquitin-independent positive regulator of the canonical NF-κB signaling pathway. It facilitates the phosphorylation of p65 by interacting with IKKα and IKKβ, promoting the p65/p50 activity and subsequent tumorigenesis [68]. In these cases, ubiquitin is not involved. Whether the remaining USPs can carry out identical regulatory mechanisms for the canonical NF-κB signaling pathway remains unknown and requires further investigation. In addition, the studies listed above can only demonstrate the quantitative correlations between the USPs and their targets but cannot explain the mechanisms clearly. For instance, no kinases interacting with USP6 were identified for p65 phosphorylation in the study of USP6-mediated p65/p50 regulation [68]. For another example, no qPCR data of IκB were provided in the study of USP14-mediated p65/p50 regulation to explain whether IκB is transcriptionally upregulated when USP14 is overexpressed [62]. These studies are rare, even though they offer certain insights into ubiquitin-independent regulatory mechanisms of the canonical NF-κB signaling pathway.

Last but not least, there are no published studies on certain USPs' role in the regulation of the canonical NF-κB signaling pathway. As they are not listed in Table 2, the functions of USP16, 17, 22-24, 26-30, 36, 37, 40-47, and 49-52 have not been studied in the USP-mediated p65/p50 regulation, leaving a major space for future exploration.

3.8.2 Implications in Human Cancers

As reviewed in 2005, the alterations of canonical NF-κB signaling pathway were found in lung, breast, ovarian, pancreatic, bladder, prostate cancer, and melanoma [15]. In this review, none of the mechanistic studies on USP-mediated p65/p50 regulation were conducted in breast cancer, ovarian cancer, and melanoma. Instead, many of the studies were conducted in leukemia monocytes and cervical cancer cells (Table 2). In addition to the cancers listed above, USP-mediated p65/p50 regulation is also found in colorectal carcinoma, renal cancer, endometrial carcinoma, and multiple myeloma (Table 2).

USP-mediated inhibition of p65/p50 activity in human cancers is usually associated with decreased malignant behaviors such as proliferation, invasion, migration, tumor formation, EMT, chemotherapy resistance, and inhibition of apoptosis. In contrast, USP-mediated promotion of p65/p50 activity in human cancers is associated with increased malignancy. These results are congruent with the findings in a review of NF-κB in human cancer [15].

If we narrow the scope down to specific cancers, such as prostate cancer only, it is apparent that there are still many investigations to be done. The four inducing pathways upstream of the IKK complex have their unique regulatory sites subject to USPs' regulation, and they converge into the IKK-p65/p50 axis (Figure 2). Despite the number of potential regulatory sites, only two studies on USP-mediated p65/p50 regulation were done in prostate cancer models, and these regulatory sites are very uncommon [41, 70]. Thus, for future prostate cancer research in this area, it will be productive to aim for the remaining potential regulatory sites (TRAF proteins, TAK1 complex, IKK complex, etc.) and screen the USPs

for each of them. This direction may also apply to future research in breast cancer, ovarian cancer, and melanoma.

4. Conclusions

According to the mechanistic studies, regulation of the canonical NF-κB signaling pathway mediated by USPs is primarily actuated through the K48-linked and K63-linked DUB activities against signaling molecules involved in the TNFR-, TLR-, and IL-1R-induced p65/p50 activation. In a few cases, the USPs can interfere with the crosstalk between PI3K/AKT and the canonical NF-κB pathway by deubiquitinating and stabilizing EGFR, PI3K, and PTEN. It has also been reported that linear polyubiquitin chains attached to NEMO and K27-linked polyubiquitin chains from TAK1 can be removed by USPs. Thus, USPs primarily function as DUBs in NF-κB regulation.

In addition, USPs regulate the canonical NF-κB signaling pathway with ubiquitin-independent mechanisms. Current studies indicate that these mechanisms involve phosphorylation of p65, ubiquitin-independent degradation of TAB2/3, and suppression of IκB expression level. These ubiquitin-independent regulatory mechanisms involving USPs are yet to be extensively studied. Given their influence on cancer cells, there is a growing need for further investigations in this area.

Based on existing findings of mechanistic studies, it is safe to draw a conclusion that future studies can be done in these aspects – removal of the K63-linked polyubiquitin chain from TAB2/3 and RIP1 by USPs, removal of atypical polyubiquitin chains from the regulatory sites (Figure 1), identifying the p65/p50-associated regulatory roles of USPs not

listed in Table 2, and ubiquitin-independent regulation of the canonical NF-κB signaling pathway mediated by USPs.

The general trend is that USP-mediated inhibition of p65/p50 activity by K63-linked DUB activity often leads to less malignant cellular behaviors of human cancers. In contrast, USP-mediated promotion of p65/p50 activity by positive-regulator-stabilization accelerates tumorigenesis (*in vivo*), colony formation, cell proliferation, invasion, and migration (*in vitro*). These changes in phenotypes due to USP-mediated p65/p60 regulation have been extensively studied in leukemia monocytes and cervical cancer models but not as extensively studied in lung, breast, ovarian, pancreatic, bladder, prostate cancers, and melanoma.

Acknowledgments

Funding: This work was supported by the National Cancer Institute at the National Institutes of Health (R01 CA255802 to Q.Z.); the University Senate Committee on Research Fellowship Program Award (to Q.Z.). The funder did not play a role in the design of the study; the collection, analysis, and interpretation of the data; the writing of the manuscript; and the decision to submit the manuscript for publication.

Figures were created with BioRender.com.

LIST OF REFERENCES

1. Wang L, Lu B, He M, et al. "Prostate Cancer Incidence and Mortality: Global Status and Temporal Trends in 89 Countries from 2000 to 2019." *Front Public Health* 10 (2022): 811044.

2. Mooney EC, Sahingur SE. "The Ubiquitin System and A20: Implications in Health and Disease." *J Dent Res* 100.1 (2021): 10-20.

3. Carroll EC, Marqusee S. "Site-Specific Ubiquitination: Deconstructing the Degradation Tag." *Curr Opin Struct Biol* 73 (2022): 102345.

4. Grice GL, Nathan JA. "The Recognition of Ubiquitinated Proteins by the Proteasome." *Cell Mol Life Sci* 73.18 (2016): 3497-3506.

5. Madiraju C, Novack JP, Reed JC, Matsuzawa SI. "K63 Ubiquitination in Immune Signaling." *Trends Immunol* 43.2 (2022): 148-162.

6. Yang Q, Zhao J, Chen D, Wang Y. "E3 Ubiquitin Ligases: Styles, Structures and Functions." *Mol Biomed* 2.1 (2021): 23.

7. Hayden MS, Ghosh S. "Regulation of Nf-Kappab by Tnf Family Cytokines." *Semin Immunol* 26.3 (2014): 253-266.

8. Zhou Z, Song X, Kang R, Tang D. "The Emerging Role of Deubiquitinases in Cell Death." *Biomolecules* 12.12 (2022).

9. Lange SM, Armstrong LA, Kulathu Y. "Deubiquitinases: From Mechanisms to Their Inhibition by Small Molecules." *Mol Cell* 82.1 (2022): 15-29.

10. Chen S, Liu Y, Zhou H. "Advances in the Development Ubiquitin-Specific Peptidase (Usp) Inhibitors." *Int J Mol Sci* 22.9 (2021).

11. Taniguchi K, Karin M. "Nf-Kappab, Inflammation, Immunity and Cancer: Coming of Age." *Nat Rev Immunol* 18.5 (2018): 309-324.

12. Rasmi RR, Sakthivel KM, Guruvayoorappan C. "Nf-Kappab Inhibitors in Treatment and Prevention of Lung Cancer." *Biomed Pharmacother* 130 (2020): 110569.

13. Zhang L, Ludden CM, Cullen AJ, et al. "Nuclear Factor Kappa B Expression in Non-Small Cell Lung Cancer." *Biomed Pharmacother* 167 (2023): 115459.

14. Zheng W, Wang X, Yu Y, et al. "Circrnf10-Dhx15 Interaction Suppressed Breast Cancer Progression by Antagonizing Dhx15-Nf-Kappab P65 Positive Feedback Loop." *Cell Mol Biol Lett* 28.1 (2023): 34.

15. Dolcet X, Llobet D, Pallares J, Matias-Guiu X. "Nf-Kb in Development and Progression of Human Cancer." *Virchows Arch* 446.5 (2005): 475-482.

16. Yu H, Lin L, Zhang Z, et al. "Targeting Nf-Kappab Pathway for the Therapy of Diseases: Mechanism and Clinical Study." *Signal Transduct Target Ther* 5.1 (2020): 209.

17. Yu C, Wang D, Yang Z, Wang T. "Pharmacological Effects of Polyphenol Phytochemicals on the Intestinal Inflammation Via Targeting Tlr4/Nf-Kappab Signaling Pathway." *Int J Mol Sci* 23.13 (2022).

18. Wang J, Wu X, Jiang M, Tai G. "Mechanism by Which Traf6 Participates in the Immune Regulation of Autoimmune Diseases and Cancer." *Biomed Res Int* 2020 (2020): 4607197.

19. Verstrepen L, Bekaert T, Chau TL, et al. "Tlr-4, Il-1r and Tnf-R Signaling to Nf-Kappab: Variations on a Common Theme." *Cell Mol Life Sci* 65.19 (2008): 2964-2978.

20. Xu G, Tan X, Wang H, et al. "Ubiquitin-Specific Peptidase 21 Inhibits Tumor Necrosis Factor Alpha-Induced Nuclear Factor Kappab Activation Via Binding to and Deubiquitinating Receptor-Interacting Protein 1." *J Biol Chem* 285.2 (2010): 969-978.

21. Tzimas C, Michailidou G, Arsenakis M, et al. "Human Ubiquitin Specific Protease 31 Is a Deubiquitinating Enzyme Implicated in Activation of Nuclear Factor-Kappab." *Cell Signal* 18.1 (2006): 83-92.

22. Xiao N, Li H, Luo J, et al. "Ubiquitin-Specific Protease 4 (Usp4) Targets Traf2 and Traf6 for Deubiquitination and Inhibits Tnfalpha-Induced Cancer Cell Migration." *Biochem J* 441.3 (2012): 979-986.

23. Dhingra R, Rabinovich-Nikitin I, Rothman S, et al. "Proteasomal Degradation of Traf2 Mediates Mitochondrial Dysfunction in Doxorubicin-Cardiomyopathy." *Circulation* 146.12 (2022): 934-954.

24. Ha J, Kim M, Seo D, et al. "The Deubiquitinating Enzyme Usp20 Regulates the Tnfalpha-Induced Nf-Kappab Signaling Pathway through Stabilization of P62." *Int J Mol Sci* 21.9 (2020).

25. Ciesielska A, Matyjek M, Kwiatkowska K. "Tlr4 and Cd14 Trafficking and Its Influence on Lps-Induced Pro-Inflammatory Signaling." *Cell Mol Life Sci* 78.4 (2021): 1233-1261.

26. Niebuhr M, Schorling K, Heratizadeh A, Werfel T. "Staphylococcal Alpha-Toxin Induces a Functional Upregulation of Tlr-2 on Human Peripheral Blood Monocytes." *Exp Dermatol* 24.5 (2015): 381-383.

27. McHeik S, Al-Akl NS, Abdelnoor AM. "The Effect of Denatured Flagellin on Toll-Like Receptor-5 (Tlr-5) in Mice." *Endocr Metab Immune Disord Drug Targets* 18.4 (2018): 412-416.

28. Wallach T, Raden M, Hinkelmann L, et al. "Distinct Sars-Cov-2 Rna Fragments Activate Toll-Like Receptors 7 and 8 and Induce Cytokine Release from Human Macrophages and Microglia." *Front Immunol* 13 (2022): 1066456.

29. Jin Y, Zhuang Y, Dong X, Liu M. "Development of Cpg Oligodeoxynucleotide Tlr9 Agonists in Anti-Cancer Therapy." *Expert Rev Anticancer Ther* 21.8 (2021): 841-851.

30. Chattopadhyay S, Sen GC. "Dsrna-Activation of Tlr3 and Rlr Signaling: Gene Induction-Dependent and Independent Effects." *J Interferon Cytokine Res* 34.6 (2014): 427-436.

31. He X, Li Y, Li C, et al. "Usp2a Negatively Regulates Il-1beta- and Virus-Induced Nf-Kappab Activation by Deubiquitinating Traf6." *J Mol Cell Biol* 5.1 (2013): 39-47.

32. Zhou Q, Xiao Z, Zhou R, et al. "Ubiquitin-Specific Protease 3 Targets Traf6 for Deubiquitination and Suppresses Il-1beta Induced Chondrocyte Apoptosis." *Biochem Biophys Res Commun* 514.2 (2019): 482-489.

33. Yasunaga J, Lin FC, Lu X, Jeang KT. "Ubiquitin-Specific Peptidase 20 Targets Traf6 and Human T Cell Leukemia Virus Type 1 Tax to Negatively Regulate Nf-Kappab Signaling." *J Virol* 85.13 (2011): 6212-6219.

34. Zhang L, Wu JH, Jean-Charles PY, et al. "Phosphorylation of Usp20 on Ser334 by Irak1 Promotes Il-1beta-Evoked Signaling in Vascular Smooth Muscle Cells and Vascular Inflammation." *J Biol Chem* 299.7 (2023): 104911.

35. Wang W, Huang X, Xin HB, et al. "Traf Family Member-Associated Nf-Kappab Activator (Tank) Inhibits Genotoxic Nuclear Factor Kappab Activation by Facilitating Deubiquitinase Usp10-Dependent Deubiquitination of Traf6 Ligase." *J Biol Chem* 290.21 (2015): 13372-13385.

36. Luo XB, Xi JC, Liu Z, et al. "Proinflammatory Effects of Ubiquitin-Specific Protease 5 (Usp5) in Rheumatoid Arthritis Fibroblast-Like Synoviocytes." *Mediators Inflamm* 2020 (2020): 8295149.

37. Zhao XB, Ji FY, Li HR, et al. "P22077 Inhibits Lps-Induced Inflammatory Response by Promoting K48-Linked Ubiquitination and Degradation of Traf6." *Aging (Albany NY)* 12.11 (2020): 10969-10982.

38. Wang Y, Zhou L, Lu J, et al. "Ubiquitin-Specific Protease 4 Predicts an Unfavorable Prognosis and Promotes Malignant Behaviors in Vitro in Pancreatic Cancer." *Exp Cell Res* 396.2 (2020): 112317.

39. Sun D, Peng Y, Ge S, Fu Q. "Usp1 Inhibits Nf-Kappab/Nlrp3 Induced Pyroptosis through Traf6 in Osteoblastic Mc3t3-E1 Cells." *J Musculoskelet Neuronal Interact* 22.4 (2022): 536-545.

40. Lin D, Zhang M, Zhang MX, et al. "Induction of Usp25 by Viral Infection Promotes Innate Antiviral Responses by Mediating the Stabilization of Traf3 and Traf6." *Proc Natl Acad Sci U S A* 112.36 (2015): 11324-11329.

41. Islam MT, Chen FZ, Chen HC, Wahid A. "Knockdown of Usp8 Inhibits Prostate Cancer Cell Growth, Proliferation, and Metastasis and Promotes Docetaxel's Activity by Suppressing the Nf-Kb Signaling Pathway." *Front Oncol* 12 (2022): 923270.

42. Fattahi S, Amjadi-Moheb F, Tabaripour R, et al. "Pi3k/Akt/Mtor Signaling in Gastric Cancer: Epigenetics and Beyond." *Life Sci* 262 (2020): 118513.

43. Glaviano A, Foo ASC, Lam HY, et al. "Pi3k/Akt/Mtor Signaling Transduction Pathway and Targeted Therapies in Cancer." *Mol Cancer* 22.1 (2023): 138.

44. Man X, Piao C, Lin X, et al. "Usp13 Functions as a Tumor Suppressor by Blocking the Nf-Kb-Mediated Pten Downregulation in Human Bladder Cancer." *J Exp Clin Cancer Res* 38.1 (2019): 259.

45. Yang Z, Xian H, Hu J, et al. "Usp18 Negatively Regulates Nf-Kappab Signaling by Targeting Tak1 and Nemo for Deubiquitination through Distinct Mechanisms." *Sci Rep* 5 (2015): 12738.

46. Fan YH, Yu Y, Mao RF, et al. "Usp4 Targets Tak1 to Downregulate Tnfalpha-Induced Nf-Kappab Activation." *Cell Death Differ* 18.10 (2011): 1547-1560.

47. Liang L, Fan Y, Cheng J, et al. "Tak1 Ubiquitination Regulates Doxorubicin-Induced Nf-Kappab Activation." *Cell Signal* 25.1 (2013): 247-254.

48. Hu B, Ge C, Zhu C. "Ubiquitin-Specific Peptidase 18 Negatively Regulates and Inhibits Lipopolysaccharide-Induced Sepsis by Targeting Transforming Growth Factor-Beta-Activated Kinase 1 Activity." *Int Immunol* 33.9 (2021): 461-468.

49. Lei CQ, Wu X, Zhong X, et al. "Usp19 Inhibits Tnf-Alpha- and Il-1beta-Triggered Nf-Kappab Activation by Deubiquitinating Tak1." *J Immunol* 203.1 (2019): 259-268.

50. Mao H, Wang M, Cao B, et al. "Interferon-Stimulated Gene 15 Induces Cancer Cell Death by Suppressing the Nf-Kappab Signaling Pathway." *Oncotarget* 7.43 (2016): 70143-70151.

51. Gong Y, Kong B, Shuai W, et al. "Usp38 Regulates Inflammatory Cardiac Remodeling after Myocardial Infarction." *Clin Sci (Lond)* 137.21 (2023): 1665-1681.

52. Zhou Q, Cheng C, Wei Y, et al. "Usp15 Potentiates Nf-Kappab Activation by Differentially Stabilizing Tab2 and Tab3." *FEBS J* 287.15 (2020): 3165-3183.

53. Li T, Guan J, Li S, et al. "Hscarg Downregulates Nf-Kappab Signaling by Interacting with Usp7 and Inhibiting Nemo Ubiquitination." *Cell Death Dis* 5.5 (2014): e1229.

54. Niu J, Shi Y, Xue J, et al. "Usp10 Inhibits Genotoxic Nf-Kappab Activation by Mcpip1-Facilitated Deubiquitination of Nemo." *EMBO J* 32.24 (2013): 3206-3219.

55. Tang X, Weng R, Guo G, et al. "Usp10 Regulates Macrophage Inflammation Responses Via Stabilizing Nemo in Lps-Induced Sepsis." *Inflamm Res* 72.8 (2023): 1621-1632.

56. Zhao W, Xin L, Tang L, et al. "A Positive Feedback Loop between Linc01605 and Nf-Kappab Pathway Promotes Tumor Growth in Nasopharyngeal Carcinoma." *RNA Biol* 19.1 (2022): 482-495.

57. Sun W, Tan X, Shi Y, et al. "Usp11 Negatively Regulates Tnfalpha-Induced Nf-Kappab Activation by Targeting on Ikappabalpha." *Cell Signal* 22.3 (2010): 386-394.

58. Schweitzer K, Bozko PM, Dubiel W, Naumann M. "Csn Controls Nf-Kappab by Deubiquitinylation of Ikappabalpha." *EMBO J* 26.6 (2007): 1532-1541.

59. Li Q, Wang M, Xue H, et al. "Ubiquitin-Specific Protease 34 Inhibits Osteoclast Differentiation by Regulating Nf-Kappab Signaling." *J Bone Miner Res* 35.8 (2020): 1597-1608.

60. Quan J, Zhao X, Xiao Y, et al. "Usp39 Regulates Nf-Kappab-Mediated Inflammatory Responses through Deubiquitinating K48-Linked Ikappabalpha." *J Immunol* 210.5 (2023): 640-652.

61. Gui D, Dong Z, Peng W, et al. "Ubiquitin-Specific Peptidase 53 Inhibits the Occurrence and Development of Clear Cell Renal Cell Carcinoma through Nf-Kappab Pathway Inactivation." *Cancer Med* 10.11 (2021): 3674-3688.

62. Li M, Zhao J, Jia L. "Usp14-Mediated Ikappabalpha Degradation Exacerbates Nf-Kappab Activation and Il-1beta-Stimulated Chondrocyte Dedifferentiation." *Life Sci* 218 (2019): 147-152.

63. Gong X, Jia L, Zhou L, Hu T. "Usp14 Predicts Poorer Survival Outcomes and Promotes Tumor Progression in Endometrial Carcinoma by Activating Nf-Kappab Signaling." *Aging (Albany NY)* 15.21 (2023): 12120-12135.

64. Colleran A, Collins PE, O'Carroll C, et al. "Deubiquitination of Nf-Kappab by Ubiquitin-Specific Protease-7 Promotes Transcription." *Proc Natl Acad Sci U S A* 110.2 (2013): 618-623.

65. Zhou L, Jiang H, Du J, et al. "Usp15 Inhibits Multiple Myeloma Cell Apoptosis through Activating a Feedback Loop with the Transcription Factor Nf-Kappabp65." *Exp Mol Med* 50.11 (2018): 1-12.

66. Schweitzer K, Naumann M. "Csn-Associated Usp48 Confers Stability to Nuclear Nf-Kappab/Rela by Trimming K48-Linked Ub-Chains." *Biochim Biophys Acta* 1853.2 (2015): 453-469.

67. Mirra S, Sanchez-Bellver L, Casale C, et al. "Ubiquitin Specific Protease Usp48 Destabilizes Nf-Kappab/P65 in Retinal Pigment Epithelium Cells." *Int J Mol Sci* 23.17 (2022).

68. Pringle LM, Young R, Quick L, et al. "Atypical Mechanism of Nf-Kappab Activation by Tre17/Ubiquitin-Specific Protease 6 (Usp6) Oncogene and Its Requirement in Tumorigenesis." *Oncogene* 31.30 (2012): 3525-3535.

69. Verstrepen L, Carpentier I, Verhelst K, Beyaert R. "Abins: A20 Binding Inhibitors of Nf-Kappa B and Apoptosis Signaling." *Biochem Pharmacol* 78.2 (2009): 105-114.

70. Liu C, Wang L, Chen W, et al. "Usp35 Activated by Mir Let-7a Inhibits Cell Proliferation and Nf-Kappab Activation through Stabilization of Abin-2." *Oncotarget* 6.29 (2015): 27891-27906.

BIOGRAPHY (VITA)

Mr. Keyi Shen was born in Nanjing, China, on February 17, 1999. He was raised by his father, Fan Shen, and mother, Xiaohong Hu. After graduating from Nanjing Zhonghua High School in 2017, he pursued his Bachelor of Science degree in Biochemistry and Molecular Biology at the University of California, Davis (UC Davis), Davis, CA, USA. He graduated from UC Davis in 2021 and joined the Master of Science program in Anatomy Research in the Department of Structural and Cellular Biology at Tulane University School of Medicine in 2022. He received training in research from Dr. Qiuyang Zhang and Zhang Lab members.